



NIAC Phase I Final Report for NNX15AL85G:
In-Space Production of Storable Propellants

Deep Space Industries Inc.

John S. Lewis, P. I.

1 March 2016

Table of Contents

Overview and Conclusions.....	1
Introduction	5
1. Available Feedstock on C-cadre Asteroids	5
2. Energy Requirements for Heating Feedstock	6
3. Recovered Water and its Uses	16
4. Electrolysis of Water for STP or Direct Combustion.....	17
5. Electrolysis of Water for Manufacture of Storables.....	19
6. Where Should we Make Propellants?	20
7. Storage and Transportation of Water and Carbon Dioxide	20
8. Methanol/Dimethyl Ether Synthesis	22
9. Conventional (Earthsided) H ₂ O ₂ Synthesis	24
10. Space-based direct synthesis of H ₂ O ₂	25
11. Long-Term Storage of Hydrogen Peroxide.....	26
12. Effect of Peroxide Degradation on Propellant Performance	28
13. Freezing and Distillation Behavior of Hydrogen Peroxide	28
14. Raw Materials Requirements for Storable Propellant Synthesis	30
15. DME/H ₂ O ₂ Combustion	32
16. Schematic Processing System Architecture on an Asteroid.....	33
17. Schematic Processing System Architecture in Earth Orbit	37
18. Hydrogen peroxide as a monopropellant	42
19. Applications of this Propellant Manufacturing Scheme: the Mars System and the Moon.....	42
20. Mission Opportunities for Use of Storable Space-based Propellants	43
20.1 Transportation from NEAs to Earth’s vicinity	44
20.2 Capture and delivery to HEEO Processing Facility orbit via single lunar swingby.....	47
20.3 Selection of the HEEO Processing and Storage Facility Orbit	50
20.4 Delivery of processed propellants to customer orbits.....	51
21. Synergy with New-Generation Low-Cost Earth-Launch Technologies.....	55
22. Terrestrial applications of improved H ₂ O ₂ syntheses	55
References	56

List of Tables

Table 1. Potential fuel/oxidizer pairs compared to feedstock composition	31
Table 2. Heats of combustion for assorted fuel/oxidizer pairs	32
Table 3. Analysis of producing different fuels for use with HTP	41
Table 4. ΔV costs (impulsively modeled) for delivery of HEEO materials to markets in other orbits	51

List of Figures

Fig. 1 Decomposition pressures of various hydrous mineral phases	10
Fig. 2 Projection of the Fe-S-O phase diagram on the p(s ₂)-p(O ₂) plane at 800 K	12
Fig. 3 Projection of the Fe-S-O phase diagram on the p(s ₂)-p(O ₂) plane at 1000 K	13
Fig. 4 The equilibrium stability field of CO ₂ clathrate hydrate	21
Fig. 5 Rate of decomposition of HTP H ₂ O ₂ in Al-alloy tanks.....	27
Fig. 6 Equilibrium phase diagram of the H ₂ O ₂ -H ₂ O system on the p(H ₂ O ₂)-p(H ₂ O) plane	29
Fig. 7 Analysis of at-the-asteroid processing identified 13 major phases.....	35
Fig. 8 The synthesis of HTP and a fuel (TBD) will be conducted in Earth orbit.....	40
Fig. 9 Ballistic Trajectory between 2009 HC and Earth	46
Fig. 10 STP transfer between 2009 HC and Earth. $I_{sp} = 200$ s, Thrust = 45N @ 1 AU	46
Fig. 11 STP transfer between 1998 KY26 and Earth. $I_{sp} = 200$ s, Thrust = 80N @ 1 AU	47
Fig. 12. Lunar swingby trajectory	48
Fig. 13 “Porkchop” Plot Showing Mission Opportunity in terms of ΔV	54

Overview and Conclusions

Our exploration of the feasibility of in-space production of storable propellants from resources available on asteroids, and also on Mars and the Moon, has considered the process of sample acquisition; the energy requirements for heating and volatile release; the thermodynamic behavior of gas release from minerals and organic polymers containing hydrogen, oxygen, carbon, sulfur, and nitrogen; purification of the released water and carbon dioxide; the storage and transportation of these materials in the condensed state; synthesis of fuels including methanol and dimethyl ether (DME); and the co-production, concentration, stability, and storage of the complementary oxidizer high-test hydrogen peroxide (HTP). We call attention to the ability of the storable propellant/oxidizer combination of DME and HTP to carry out deep-space missions and to perform retrieval and relocation of any and all space-derived resources, such as retrieving asteroidal metal to high Earth orbit. This study's analyses are based on returning resources to a storage/processing/dispensing facility in a Highly Eccentric Earth Orbit (HEEO) with a perigee above geosynchronous orbit and an apogee approach or beyond the Moon's orbit.

The methane/LOX option, notable for good engine performance, has not been included in this study because our scope includes only fully storable propellants.

This work in Phase I has led to a number of conclusions. These are:

1. Thermodynamic theory shows that extraction of water and carbon dioxide from carbonaceous (C-type) near-Earth asteroids by means of direct solar heating is feasible and efficient. This is in agreement with experiments carried out by Joel Sercel in an independent NIAC Phase I project, using both CM type meteorite material and a C-type asteroid simulant that we have developed at DSI and the University of Central Florida under an SBIR grant running concurrently with this (and his) NIAC grant.
2. The same theory also predicts that attempts at full extraction of volatiles from a C asteroid will require calciner temperatures of at least 700 K, at which temperature not only does the native organic polymer in the C asteroid material react with magnetite (Fe_3O_4) to generate carbon dioxide and water vapor, but also these gases react with coexisting sulfide and sulfate minerals to release copious amounts of sulfur dioxide. This prediction has also been qualitatively verified by Joel Sercel's work on meteorite and DSI simulant materials. At these temperatures, release of H, C, O, N, and S produces gases amounting to about 40% of the total mass of the asteroidal material.
3. The principal sulfur gas released, sulfur dioxide, is a source of some concern for several reasons. It is a toxic and offensively odorous gas that must be removed from water intended for life-support or hydroponic use. It also spontaneously generates elemental sulfur and sulfuric acid, highly undesirable materials that can corrode or clog water-handling systems such as Solar Thermal Propulsion engines. Further, some of these sulfur compounds can poison the catalyst beds used in several critical processing steps in manufacture of propellants and metal products.

4. Sulfur impurities may be removed on the asteroid from freshly generated impure water to make it safe and suitable for these uses. The application of Reverse Osmosis (RO) or other relevant technology provides the requisite purification in a simple and safe manner, using equipment of high TRL. The purified water is then suitable for use in everything from STP thrusters to chemical reagents to chemical propellant manufacture to life-support fluids.

(4alt.) Alternatively, SO₂ release may be minimized by using lower calcining temperatures, which also severely limits CO₂ release. This option suggests retrieval of only water to HEO on the first mission, with production of only H/O propellants. Such a mission would also provide an opportunity for retrieval of unprocessed asteroid material to HEEO for use in process-development experiments there, relegating CO₂ and SO₂ production to HEEO.

5. The “rejected” sulfur compounds from water purification are a valuable feedstock for manufacture of industrial grade sulfuric acid, a critically important and useful chemical reagent for mineral and metallurgical use, and do not represent waste. We have not yet studied the handling and processing of this sulfur-rich material since it is not the main focus of this project; for present purposes we envision sequestration and storage of sulfuric acid against future demands. In scenario 4, the sulfuric acid would be made and stored on the asteroid; in scenario 4alt this would take place on the HEEO facility.

6. Manufacture of HTP and DME (or methanol) requires only CO₂ and H₂O as raw materials, in the proportion of 2 CO₂ molecules per 9 molecules of H₂O for making DME/HTP (1:5 for methanol/HTP). Several candidate processes are available for manufacture of each product, all requiring the presence of hydrogen and oxygen gas. Thus electrolysis of water is an essential step in storable propellant manufacture. This process is carried out routinely as part of the life support (oxygen recovery) system of the International Space Station, and has a very high TRL, with years of flight experience.

7. CO₂ and H₂O can be co-condensed as a methane clathrate hydrate, CO₂·6.75H₂O, close in composition to the desired ratio for coproduction of HTP and DME, with some excess water. Hydrate formation appears to be a very useful way of storing and transporting its component gases for in-space industrial use, and may be a patentable process. If clathrate formation proves too challenging in our Phase II laboratory tests, transport as solid CO₂ and H₂O is feasible.

8. Production of methanol can be effected by passing a mixture of hydrogen and carbon oxides (either CO or CO₂) through any of several types of industrially validated catalyst beds. DME can be produced efficiently either by dehydration of methanol (one common practice is dehydration of methanol by reaction with sulfuric acid) or using a two-layer catalyst bed with the methanol product being immediately passed at higher pressure through a gamma-alumina catalyst layer to manufacture DME. Either methanol or DME is a credible propellant.

9. Most terrestrial manufacturing schemes for HTP use organic catalysts of questionable utility in space; however, one proposed (and partially patented) scheme is simply an adaptation of conventional H₂O fuel cell technology optimized for HTP production rather than electrical energy generation. Further development of this scheme and validation of various candidate electrode materials looks very promising for efficiency, robustness, and simplicity.
10. The essential on-asteroid processing steps and flow diagrams (heating, condensation, reverse osmosis, and freezing for transport) seem readily manageable, whereas the ensuing processing steps for co-production of HTP and DME are a mixture of high-TRL and low-TRL steps of a higher degree of complexity. It would seem prudent to carry out these steps in near-Earth space where human-tended or tele-operated equipment would carry out the synthesis.
11. HTP production in this scheme is remarkably free of sources of contaminants that could catalytically destroy HTP during storage. We have developed a quantitative model of the kinetics of HTP decomposition that shows extremely low decomposition rates (order of 10^{-4} to 10^{-5} %/year) when stored in appropriate containers near or below the freezing point with ppm concentrations of sodium or potassium stannate as stabilizer.
12. The insensitivity of propellant performance (for example, the I_{sp} for DME/HTP fueling) on the water content of HTP makes extreme purification of the HTP to <5% H₂O unnecessary.
13. It appears that the best system architecture would involve water production and purification at the asteroid, use of STP with water as the working fluid for the retrieval of large masses of asteroidal material to Earth orbit, and processing of retrieved water and carbon dioxide in Earth orbit to manufacture storable (or cryogenic) propellants for use in outbound missions to asteroids or any other destination.
14. C asteroid processing schemes (but not sample acquisition schemes) would be applicable to any source of CO₂ and H₂O, including lunar polar volatiles and Martian volatiles.
15. Whether future missions will employ deep cryogenics (LH₂/LOX), mild cryogenics (methane/LOX), storables, or simply water for STP or NTP use, retrieval and purification of asteroidal volatiles (water and carbon dioxide) is a key technology.
16. Water-based STP, with its low power (governed by the solar flux), has sufficient I_{sp} (at least 200 s) to serve well for launching a water payload from an asteroid and directing it to Earth intercept, but lacks the acceleration to be effective in capturing into Earth orbit at approach speeds too high for lunar capture. Chemical propulsion, with its high thrust level, is better suited for both Earth capture (via inverse Oberth effect at low altitude) and Earth departure to deep-space targets. Initially, carrying some of the propellant derived from earlier missions to assist in Earth capture may be desirable.

16alt. In the same way, Earth capture via aerobraking with or without a lunar swingby is an extremely promising way to improve overall performance (mass payback ratio) of the system. Aerobrake manufacture and use are not within the scope of this study.

17. Looking forward, manufacture of propellants at the asteroid target will require significant experience in Earth orbit to validate and fully automate the processes, suggesting that it will be significantly farther downstream and that current research should concentrate on improving the low-TRL parts of the processing scheme in Earth orbit.

18. Development of the technologies for in-space propellant manufacture can easily be approached as a stepwise, evolutionary sequence. The logical sequence appears at present to be:

- a) Extraction of water from an NEA and return to Earth orbit via Solar Thermal Propulsion using part of the water as the STP working fluid. All water processing into marketable products would occur in HEEO. Products available in Earth orbit would include water, hydrogen, oxygen, and hydrogen peroxide, addressing markets such as radiation shielding (water), life support (water and O₂), cryogenic propellants (LOX/LH₂), and monopropellants for station-keeping and microsatellite propulsion (H₂O₂). Critical technologies include water extraction and purification, development of a water-based STP system, adaptation of ISS water-electrolysis technology, and production of high-test peroxide (>95% purity H₂O₂; HTP). If deep-cryogen propellants are desired, then liquefaction of oxygen and hydrogen are required.
- b) Extraction of carbon dioxide from the same NEA and return of water and CO₂ via water-based STP to HEEO, quite possibly transporting these materials as a solid clathrate hydrate. With water and carbon dioxide available as feedstocks, carbon-based storable propellants such as dimethyl ether (DME) or methanol (CH₃OH) can be co-produced with hydrogen peroxide. Results from Phase I indicate that the first missions actually may be able start with this phase – combined water and CO₂ harvesting – and a critical part of the Phase II research is verifying that this leap is feasible.
- c) Using the same starting materials, methane/LOX production in HEEO becomes possible. This is an attractive intermediate between deep cryogenics (LH₂) and fully storable propellants (HTP/DME) in terms of both technical difficulty and performance.

19. In the longer run, once experience in storable propellant manufacture is in hand, it would be desirable to transfer that process to the surface of the asteroid where mining and extraction are taking place. This would open up a variety of new mission opportunities to, for example, Belt asteroids and the outer planets.

Introduction

The idea of using asteroidal materials as an economic resource can be traced back to the writings of Konstantin Tsiolkovskii in 1903 and Robert Goddard in 1908, although without any details or examples of such processes and uses. The extraction of materials, notably water, from carbonaceous near-Earth asteroids (NEAs) for propellant manufacture was explored in the 1990s^{1,2} in sufficient detail to generate substantial interest in the process. In parallel, numerous studies of the orbital and thermal evolution of Jupiter family (short-period) comets established the principle that many bodies in the NEA population may be ice-rich dormant comets with dirty-ice cores, shielded by a “lag deposit” of fluffy, opaque, poorly conductive carbonaceous dust with a thickness of one to several meters, left behind by evaporation of near-surface ices during multiple perihelion passages. The literature on this subject has been ably reviewed by Weissman, et al.³ Several studies by Eugene Shoemaker, Richard Binzel, and other asteroid experts have proposed that 40 to 60% of the NEAs may be former short-period comets, each of which in turn may contain 60 to 80% readily extracted volatiles. Such extinct or dormant comets would be extremely dark, spectrally similar to carbonaceous chondrite meteorites, due to the lag deposit of carbonaceous dust coating their surfaces. Thus an “asteroidal” target may well be a rich source of cometary volatiles.

1. Available Feedstock on C-cadre Asteroids

There are several classes of very dark asteroids in the near-Earth population, collectively referred to as the C-cadre asteroids. These include the B, C, D, F, G, P and T spectral types. All are very dark, with albedos (reflectivities) in the range 0.10 down to 0.023), and some show an absorption feature in the 3 μm spectral region due to water. Of these asteroid types, only one is well-represented by meteorite samples: the spectra of the C asteroids correspond closely to those of the CI and CM carbonaceous chondrite meteorites. The unique Tagish Lake meteorite may also be a spectral match for the D asteroids, many of which have orbits indistinguishable from those of short-period Jupiter-family comets. The Almahatta Sitta meteorite, which fell in the Sudan in 2008, was observed astronomically before impact, and indeed the impact was predicted based on a short run of tracking data on it in its short career as a known NEA, cataloged as 2008 TC₃. The spectrum measured during its approach to impact was found to resemble the F-type asteroids. Most of the material recovered from this fall belongs to the very dark ureilite achondrite family of meteorites, which are quite dry but contain up to 3% by mass carbon.

Most dark asteroids belong to the C type, which are notable for a highly disequilibrium low-temperature mixture of minerals of very diverse formation conditions. This asteroid spectral type corresponds to the CI and CM meteorite classes, which contain 5 to over 20% by weight chemically bound water and 3 to 6% black polymeric organic matter. They also contain about 6% sulfur, including sulfides, sulfates, elemental sulfur and organic sulfur, plus abundant magnetite

containing extractable oxygen totaling about 12% of the meteorite mass. The CI chondrites contain a grand total of about 40% by weight extractable H-C-O-N-S volatiles.

Astronomical observations⁴ of comet 67P/Churyumov-Gerasimenko made several years before Rosetta's arrival found the albedo of its nucleus to be 0.04 ± 0.01 . The recent Rosetta⁴ mission observations have found a global average albedo of 0.06 ± 0.01 just before perihelion passage. This is of course not compatible with fresh ices, but is entirely compatible with the surface being dominated by a lag deposit of C-type material.

The B, G and T asteroid spectral types appear to be thermally altered C material, but unfortunately are without convincing representation in our meteorite collections. The T and D asteroids, however, are known to be common among the NEAs whose orbits are most similar to those of short-period comets. The P asteroids are very common at the outer edge of the asteroid belt, but none are known in the NEA swarm.

In addition to these unambiguously dark objects, there are many asteroids that are assigned to the X type. These are objects for which there are no albedo data, but the spectrum is known to be quite flat and featureless. The spectral types compatible with the X-type designation include the very bright E-type asteroids, the moderately-bright M type (metallic) asteroids, and the very dark D-type (cometary) bodies. The large X-type NEA 2013 UQ4, roughly 10 km in diameter, is in a retrograde orbit with a perihelion at 1.08 AU. Its reported albedo is 0.04, which, if verified by other observations, is compatible with it being both a short-period comet and a D-type NEA. It is a member of the Damocloid family of dormant Jupiter-family comet nuclei, of which at least 60 have been identified, only five of which approach closely enough to the Sun to qualify as NEAs. The type example, 5335 Damocles, formerly 1991 DA, has a perihelion of 1.58 AU and is not presently an NEA, although numerical integration of its orbit suggests that it should spend about 25% of its time in Earth-crossing orbit.

2. Energy Requirements for Heating Feedstock

Water and carbon dioxide, the essential and dominant carriers of H, C, and O in carbonaceous asteroids, must be released from their parent asteroid regolith by solar heating. The released gases are complex in composition, reflecting temperature, time, heating rate, gas back-pressure, and the kinetics of poorly-understood chemical reactions.

Energy is absorbed during the process of baking the regolith, partially as heating of the solids ($C_p\Delta T$) and partially as the heat of decomposition (water vaporization) of the phyllosilicate ($\Delta H^{\circ}_{\text{vap}}$). Both numbers vary slowly with temperature, and vary in opposite senses. Uncertainties in predicting gas release profiles (emitted gas flux and composition vs. temperature during heating) are introduced by the complex nature of, and lack of thermodynamic data on, the organic polymer and by the poorly characterized phyllosilicates, which commonly exhibit a diffuse X-ray powder

pattern implying a wide range of structures, compositions, and thermodynamic properties (i.e., water vapor pressure) of coexisting, and probably interleaved, layer-lattice silicates.

Thermodynamic calculations on the release of volatiles from heated CI material are only suggestive because true equilibrium is not attained in the time/temperature regime of interest; nonetheless H₂O, CO₂, and SO₂ are produced along with a few percent H₂S (H₂S/H₂O = 0.03) and a fraction of a percent of H₂ (H₂/H₂O = 0.003 at 1200K (927 °C)). Of these gases, the ones of greatest immediate economic interest and utility are water vapor and carbon dioxide. There is reason to prefer relatively low-temperature (below 700 K) extraction of water vapor to avoid the complications introduced by the vapor chemistry of sulfur, however at this lower temperature carbon dioxide release is also lower.

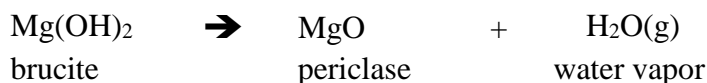
The principal sources of thermodynamic data on reactants and products used herein are the JANAF Thermochemical Tables⁵ (principally for gases), Domalski's⁶ tables (for organic compounds), and Robie and Hemingway's⁷ U. S. G. S. Bulletin 2131 (for the thermodynamic properties of minerals). A set of detailed process simulations has also been conducted by our collaborator Sam Spencer (examples included later in this report) using mining/oil/gas industry-grade process- modeling software, namely SysCAD v9.2 (<http://www.syscad.net/>) and HSC v5 for thermodynamic data (<http://www.outotec.com/en/Products--services/HSC-Chemistry/>). For the results of these simulations, see Section 17.

Water: Heating bulk CI material from ambient asteroidal surface temperatures (about 200 K) to the point at which large-scale evolution of water vapor occurs (about 700-800 K) depends on the heat capacity of the bulk solids, which we estimate as roughly 1200 J/kg·K, or 720 kJ/kg, or 720 MJ/tonne. The heat of decomposition ("water vaporization") of the hydrous silicates, which must also be included, is not the usual heat of vaporization of water, but the overall enthalpy change of the reaction which releases water vapor, including all reactants and products.

The first example of water vapor release is simply the evaporation of water (sublimation of ice):

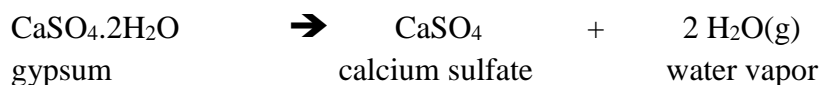
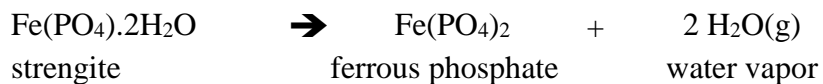


An equally simple example of a mineral decomposition reaction is the heating of brucite:

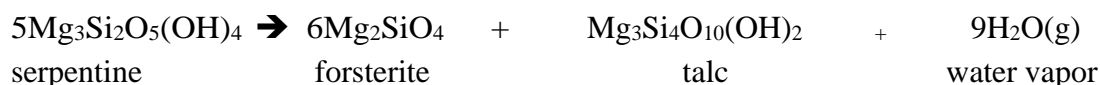


This reaction produces a water partial pressure of 1 bar at 540 K (267 °C).

Other simple dehydration reactions producing a water partial pressure of about 1 bar at 540 K (267 °C) include:

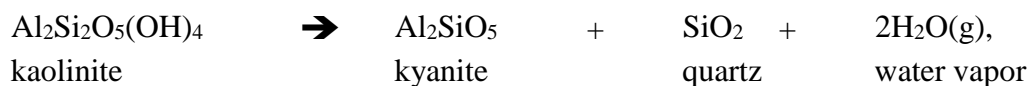


More realistic is the dehydration of serpentine (as lizardite or chrysotile) and/or of talc:



which delivers 1 bar partial pressure of water vapor at 800 K.

Typical of clay minerals is kaolinite, which decomposes to kyanite, quartz and water vapor upon heating via the reaction:



which has an enthalpy cost of 135.4 kJ mol⁻¹ of kaolinite at 800 K (thermodynamic data from USGS Bulletin 2131)⁷. This is equal to 0.52 kJ per gram of kaolinite, which is 14 % water by mass. Thus decomposition of a pure kaolinite feedstock would absorb 520 MJ per tonne and release 140 kg of water. The average heat capacity of kaolinite over the range 200-800 K is about 1.2 J/gK, or 720 MJ/tonne. Thus the total energy cost of extracting the water is 1240 MJ per tonne of solids, or 8.7 GJ per tonne of water. Much of this heat, at least 50% and perhaps 75%, can be recaptured by using the heat content of the spent solid charge and heat of condensation of water to heat incoming asteroidal material. Cooling water vapor from 800 K down to the condensation point releases about 4300/0.2392x18 J/g (1.00 GJ/tonne). The heat of condensation of liquid water at 298 K is 582 cal/g (2.43 GJ/tonne), and for direct condensation to water ice Ih, it is about 2.84 GJ/tonne at -10°C. (Total heat release from the cooling and condensing water therefore ranges from 3.4 to 3.8 GJ/tonne of water.) Heat release from the residual solids is on the order of 480 MJ/tonne solids, but the mass of spent solids is 86/14 times the mass of water, so the perfect

recovery of heat from the solids left after extraction of 1 tonne of water provides 2.85 GJ/tonne of water, giving a total heat content of about 6.5 GJ/tonne water.

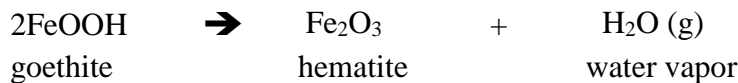
Another phyllosilicate found in CI chondrites is montmorillonite, a clay of the smectite family nominally having the formula $\text{Al}_4\text{Mg}_6(\text{Si}_4\text{O}_{10})_4(\text{OH})_8n\text{H}_2\text{O}$, which is commonly also host to variable amounts of sodium, calcium, potassium, iron and other minor cations. Sodium-bearing montmorillonites are strong absorbers of water, with very complicated and composition-dependent affinity for water and consequently with very complex water-release behavior. Montmorillonite is a voracious host of interlayer water, which leads to swelling of the clay to several times its “dry” volume. Commercial bentonite, a “swelling clay”, consists largely of montmorillonite. The water content of sodium-bearing varieties can be as high as several times the dry mass of clay. All clays in this family have a remarkable ability to exchange ions with interstitial solutions, enhancing the compositional diversity of the clays. As little as 2% montmorillonite in the CI parent body could hold enough water to account for 10% water in the total mineral mix. Most of this water would be rather loosely bound and therefore vulnerable to easy loss and to chemical and isotopic exchange with Earth’s atmosphere. The water release profile of smectite clay cannot be calculated from basic principles, and must be measured for each specific clay composition.

An important process in the history of CI chondrites was the serpentinization of the high-temperature minerals olivine and pyroxene by reaction with liquid water. Serpentine (as represented by the structurally and chemically similar minerals chrysotile, lizardite and antigorite)⁷ and coexisting brucite (or any thermodynamically compatible Mg-rich clay) would release water upon heating, reconstituting forsterite olivine:



Thermodynamic data are available for this reaction⁷ in USGS Bulletin 2131.

Poorly characterized iron oxide species in carbonaceous chondrites and C asteroids probably include goethite and maghemite (both with formula FeOOH), which decompose upon heating to release water via:



A graph of the water pressure curves for a variety of hydrous minerals is given in Fig. 1:

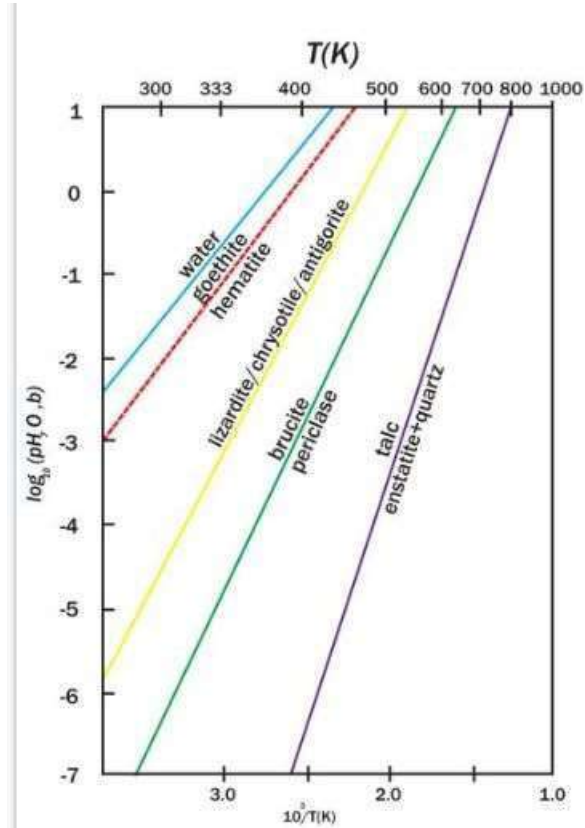


Fig. 1 Decomposition pressures of various hydrous mineral phases. The equilibrium vapor pressures over liquid water, goethite/hematite, serpentine, brucite/periclase and talc/enstatite + quartz are shown as a function of temperature. The important decomposition behavior of montmorillonite cannot be graphed because of the extreme compositional variability of the clay and the several modes of water attachment to the clay. Equilibrium is unattainable at low temperatures because of the structural complexity of CI chondrites; however, note that even at 700 K the pressures of all these water buffers lie above 1 bar (10^5 N/m^2).

The solar energy required to extract water (8.7 GJ per tonne of water) over a one-year period could be supplied by a solar reflector with a collection area sufficient to provide $8.7 \times 10^9 / 3 \times 10^7 \text{ J/s} = 290 \text{ W}$; for 1000 tonnes of water we require 290 kW continuous power. At 1 AU from the Sun, 1 m^2 of solar collector provides 1350 W; at 3.16 AU the power drops to 135 W per square meter. To produce enough thermal power to generate 1000 tonnes of water in one year at 3.16 AU requires 2150 m^2 of collector area, a circle 52 meters in diameter. If the water extraction is done at 1.0 AU from the Sun (such as on a low-eccentricity NEA), a solar collector with a diameter of 17 m would suffice over one year of exposure.

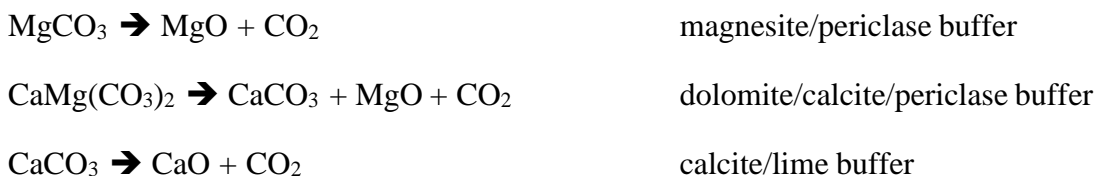
Carbon dioxide release can occur via several different reactions. First, and easiest to quantify, is the relatively minor amount of CO_2 released by thermal decomposition of carbonates⁸ such as siderite (FeCO_3), dolomite ($\text{CaMg}(\text{CO}_3)_2$) and calcite (CaCO_3).

Siderite can decompose directly upon heating by two different pathways:



Since siderite in carbonaceous meteorites coexists with magnetite, either or both of these decomposition reactions may be relevant. The thermodynamic data on siderite are incomplete and of rather low quality, making accurate calculation of the gas release behavior impossible.

Both calcium and magnesium carbonates are also found in CI chondrites, mainly as calcite and dolomite, although magnesite (MgCO_3) has also been reported. The relevant decomposition reactions are:



Strictly speaking, carbonates are usually destroyed by reaction with silica-bearing minerals via reactions that take up the highly reactive periclase and lime, schematically:

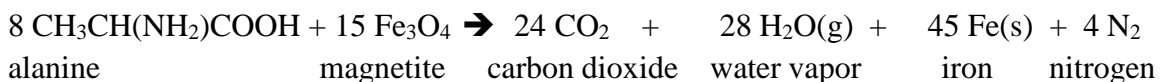


However, since there is no free silica in carbonaceous chondrites, this reaction path requires intimate contact between carbonate minerals and silicate phases from which they can extract silica with thermodynamic activities far less than 1.000 (the case of pure coexisting silica). This is generally not the case and is not considered in this study.

At higher temperatures we also have CO_2 released by the reaction of organic polymer with abundant magnetite, effectively



The latter CO_2 source cannot be modeled quantitatively at lower temperatures because of lack of both thermodynamic and kinetic data on the polymer; however, the organic polymer would char and eventually graphitize at elevated temperatures, suggesting that a graphite activity of 1.0 would be a reasonable approximation above 1000 K. Note that this process of oxidizing organic matter by reaction with magnetite also releases the sulfur and nitrogen contained in the polymer. One example of this is the oxidation of the trace amino acid alanine:



Sulfur Dioxide: With rising temperatures the mineral assemblage changes from the assemblage pyrite/pyrrhotite/magnetite/anhydrite at 800 K to pyrrhotite/magnetite/anhydrite or (with more

oxidation) pyrite/magnetite/anhydrite/magnesium sulfate at 1000 K. The equilibrium phase diagram for the relevant minerals at 800 (Fig. 2) and 1000 K (Fig. 3) in the Fe-S-O system, graphed on a format of log p_{S_2} vs log p_{O_2} , is marked with x to show the sequence of mineral changes and gas composition as a function of the degree of oxidation.

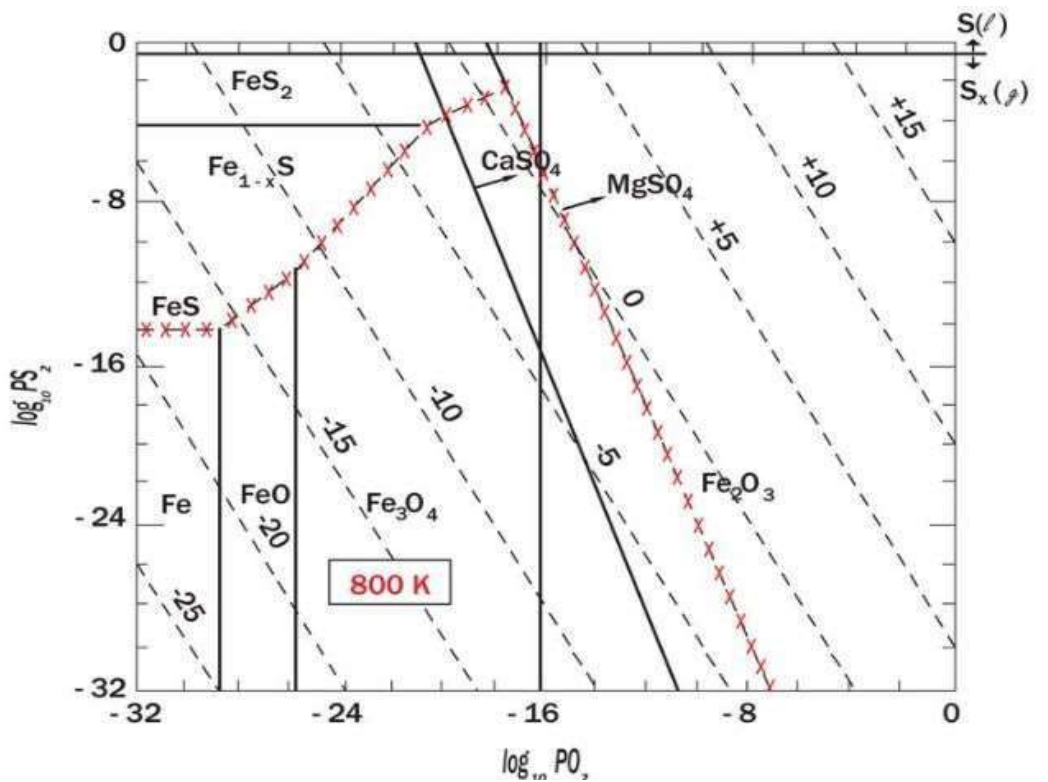


Fig. 2 Projection of the Fe-S-O phase diagram on the $p(S_2)$ - $p(O_2)$ plane at 800 K. The strong solid lines demarcate the stability fields of Fe metal (kamacite), FeO, Fe₃O₄ (magnetite), Fe₂O₃ (hematite), FeS (troilite), Fe_{1-x}S (pyrrhotite), FeS₂ (pyrite), S_l (liquid sulfur), CaSO₄ (anhydrite) and MgSO₄. The diagonal lines give contours of the log₁₀ of the equilibrium SO₂ pressure from 10⁻²⁵ b (lower left to 10¹⁵ b in the upper right). The line marked x, progressing from left to right, marks the trajectory of mineral compositions followed during sequential oxidation. Note that the sulfur vapor pressure (S₂) and the SO₂ pressure both reach maxima at the point at which magnesium sulfate first appears. The equilibrated mineral assemblage in a CI chondrite would lie near this point. Note that at 800 K the sulfur vapor pressure reaches about 0.01 b and the SO₂ pressure reaches about 10 b. Other sulfur gases including H₂S and COS may also be important.

At any relevant temperature, the SO₂ partial pressure goes through a maximum, which also occurs at the point of maximum partial pressure of sulfur vapor (S₂). Beyond 1000 K, at somewhat higher temperatures, pyrite melts incongruently at 1083 K, forming solid pyrrhotite and a liquid sulfur-rich melt. As temperatures are raised from 800 K to 1000 K all sulfur-bearing gas pressures increase: the 800 K assemblage produces about 0.01 b SO₂ and the 1000 K mineral suite yields about 0.05 b; further oxidation beyond the appearance of magnesite and disappearance of sulfides yields an abundance of S₂ vapor that is about 10% of SO₂ at the 800 K point and roughly equal to SO₂ at 1000 K.

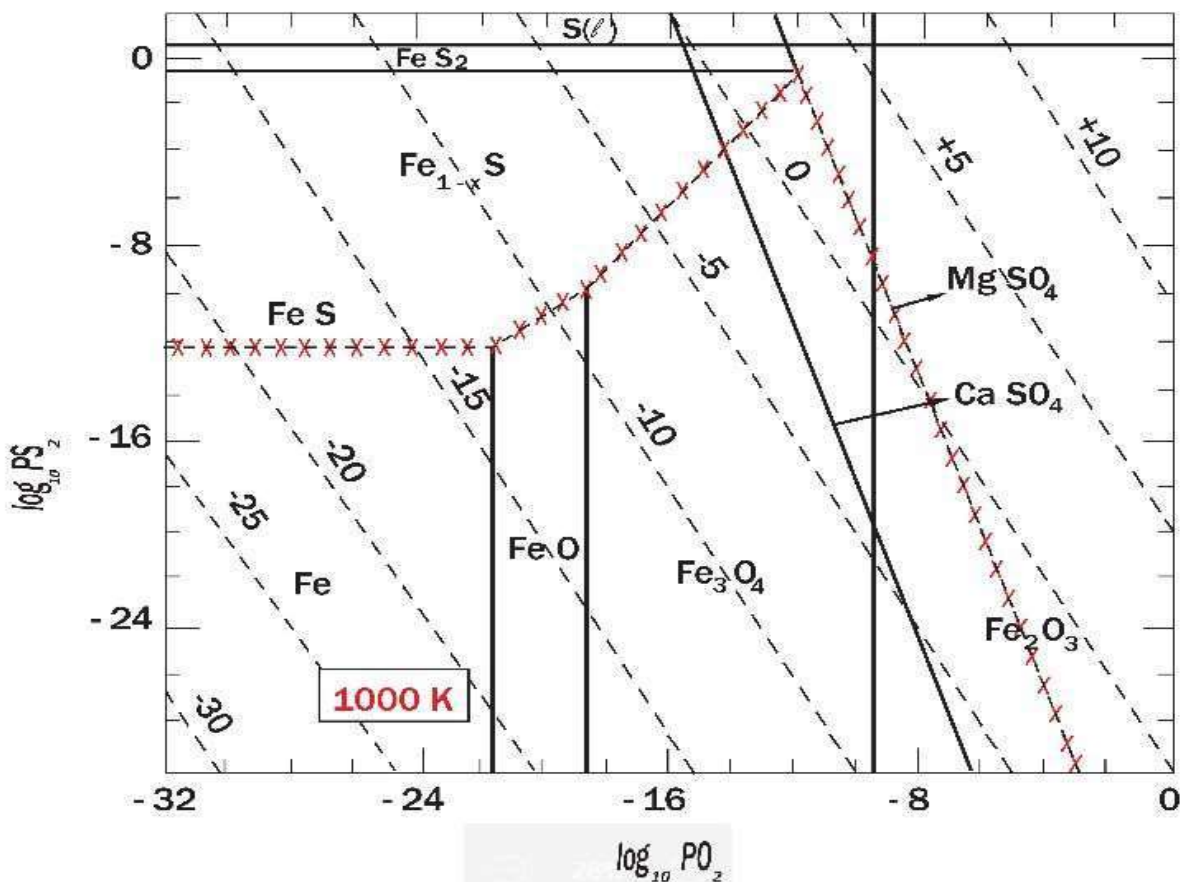


Fig. 3 Projection of the Fe-S-O phase diagram on the $p(S_2)$ - $p(O_2)$ plane at 1000 K. The strong solid lines demarcate the stability fields of minerals as in Fig. 2. The dashed lines give contours of \log_{10} of the SO_2 partial pressure in b . The peak equilibrium SO_2 pressure occurs at an oxidation state that corresponds to the coexistence of $CaSO_4$, $MgSO_4$, Fe_3O_4 and the pyrrhotite-pyrite boundary, consistent with equilibration of the minerals seen in CI chondrites. The S_2 partial pressure at that point is about $0.1 b$, compared with about $100 b$ for SO_2 .

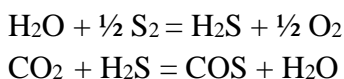
At slightly higher oxidation states the partial pressures of sulfur gases drop rapidly due to the formation of low-volatility sulfates such as anhydrite ($CaSO_4$) and $MgSO_4$. Sulfur gases are therefore likely to be significant contaminants in the water and carbon dioxide released at all temperatures. Certain sulfur gases, such as hydrogen sulfide, sulfur dioxide, carbonyl sulfide and sulfur trioxide, would impart unpleasant and even toxic smells and tastes to water. Sulfur dioxide dissolves extensively in cold water (228 grams per liter of cold water at 1 bar partial pressure of SO_2) to make the weak acid H_2SO_3 , sulfurous acid. The SO_3^{2-} (sulfite) ion in sulfurous acid is unstable and spontaneously disproportionates into sulfate and elemental sulfur:



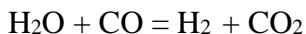
H_2SO_4 , sulfuric acid, is of course a strong acid. Disproportionation is the process by which one unstable oxidation state splits into products with both higher and lower oxidation states. It could

equally well be called a self-oxidation-reduction reaction. Here S^{4+} disproportionates into S^{6+} and S^0 (schematically, $3S^{4+} \rightarrow 2S^{6+} + S^0$). This happens spontaneously and requires no other reactant, occurring even when there is no oxidizing agent added. Certain materials act as catalysts to accelerate the disproportionation reaction. Sulfuric acid, the main product of disproportionation, is a problem because it threatens corrosion of metal plumbing, reaction vessels, tanks, etc. Any additional oxidizing agent that may be present simply accelerates the conversion of sulfite into sulfate. Elemental sulfur, most likely rhombic sulfur, can also create problems by depositing as solid sulfur dust in the gas system. Rapid quenching of a gas rich in sulfur vapor (principally S_2) causes precipitation of a glassy polymeric sulfur phase, an even worse contributor to clogging of pipes and valves. Some materials may act as catalysts and accelerate the rate of disproportionation of sulfite, but without changing the results.

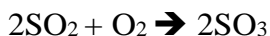
In addition to diatomic sulfur and sulfur oxides, the released gases must contain carbonyl sulfide (COS) and hydrogen sulfide (H_2S). Gas-phase equilibria of sulfur-bearing gases are generally rapid, so the equilibrium assumption for the reactions



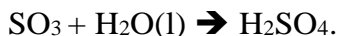
is probably an excellent approximation. These reactants are also linked by the water gas reaction,



Management of sulfur is important for four basic reasons: sulfuric acid is, as mentioned above, corrosive. Sulfur also poisons catalysts of several important chemical reactions and, as mentioned above, sulfur deposition threatens to block pipes and valves. Finally, sulfuric acid is potentially an extremely valuable industrial reagent for mineral processing and metal extraction, which creates a strong incentive to control sulfur chemistry and to conserve and manage the products. This is most easily done by complete oxidation of sulfur dioxide to sulfur trioxide,



which is removed by a wet scrubber as sulfuric acid, taking advantage of the extremely hygroscopic nature of sulfur trioxide.

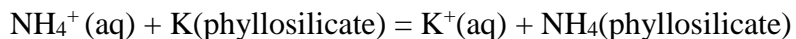


This is standard practice in terrestrial mineral industry applications. The concentrated sulfuric acid from the scrubber could be retained in an appropriate container such as Teflon-coated or chemically passivated metal for future use.

The presence of reactive sulfur gases in the gases released by any but the mildest heating presents a complicating factor that cannot be ignored. One possible means of dealing with sulfur is to electrolyze water to generate oxygen before the extracted water can be purged of sulfur compounds for safe use and storage. Whether this must be done on the asteroid is an open issue. Uncertainty in the release behavior of sulfur and carbon oxides during heating is an issue that can only be resolved experimentally, an urgent task for Phase II. Alternate means of purification of water on the asteroid must also be studied and proven experimentally.

Although combustion of sulfur compounds has been suggested by David Vaniman⁹ and coworkers for use in rocket engines, especially in the context of lunar-derived propellants, the molecular weight of the exhaust products is so high (molecular weight of 64 for SO₂; 80 for SO₃), and sulfur trioxide is so corrosive and noxious, that we must regard the use of sulfur compounds as propellants to be far less attractive than their industrial use. However, if some means of using sulfur as a propellant can be developed, it is clear that many classes of asteroidal material, which have 5-6% by mass sulfur, are vastly more amenable to this use than lunar surface materials, which average about 0.05 to 0.10% total sulfur content. Once again, as with H, C, and Fe metal, lunar concentrations of these marketable materials are typically several hundred times lower than in most meteorites and asteroids.

Nitrogen and Ammonia: The earliest studies on the freshly-fallen Orgueil CI chondrite by Cloëz¹⁰ and Pisani¹¹ in 1864 reported a strong odor of “sal ammoniac” (ammonium chloride) which quickly dissipated over time, and which was not found in analyses a century later. Thus we may find that early low-temperature gas release will produce ammonia and HCl until primordial NH₄Cl is exhausted. (NH₄Cl itself does not exist in the gas phase.) Release of nitrogen from the polymer as it is oxidized by reaction with magnetite will further complicate the issue, but ammonia will be destroyed at these temperatures and this oxidation state, generating molecular nitrogen. There is a further possibility that the ammonium ion NH₄⁺, which has the same ionic charge and virtually the same ionic radius as potassium ion K⁺, may populate alkali metal sites in phyllosilicates. The equilibrium constant for the exchange reaction:



is known to be close to 1 for a variety of host minerals, including feldspars; thus “fossil” ammonium ion may still reside in solid silicates and salts even after the loss of the much more volatile ammonium chloride. The spectral signature of ammonium ion is in the same spectral region as the 3- μm “water band”, the fundamental stretching frequency of the O-H bond. The Dawn mission’s studies of the thermally altered carbonaceous asteroid Ceres show the possible spectral signature of ammonium ion.

The organic polymer has a nitrogen content equivalent to about one N atom per 6 to 10 C atoms, totaling about 0.6% by mass of the total meteorite. Some of the nitrogen is bound in heterocyclic aromatic fragments, some as nitrile groups $-\text{CN}$, and some as amine groups $-\text{NH}_2$. Thermal deamination of the amines and decarboxylation of carboxylic acid groups will release ammonia and carbon dioxide at relatively low temperature, accompanying water release from organic $-\text{OH}$. Hydrolysis of nitriles with release of HCN, cyanogen, and possibly N_2 will occur at higher temperatures. Complete destruction (via “combustion”) of the polymer with release of structural N as N_2 requires the highest temperatures, probably close to 1000-1200 K. Oxidation appears to be an essential step to destroy HCN to make the extracted water safe for use in life-support systems. Unfortunately the speciation of N in the organic matter and the temperature release behavior of nitrogen-bearing gases are both poorly known.

Because of these uncertainties, release of these organic and inorganic nitrogen components from heated asteroidal or meteoritic material cannot be modeled with existing data except in the high-temperature limit of complete gas release, under conditions closely approaching equilibrium, where the N_2 partial pressure should approach 5% of the CO_2 pressure.

For study purposes the only current source of nitrogen in the C asteroid regolith is assumed to be the organic polymers (see carbon dioxide release).

3. Recovered Water and its Uses

As we have seen, there is good reason to suspect that significant traces of sulfur and nitrogen compounds may be present among the gases released by heating C asteroid material. At present, the presence of these minor constituents does not appear to compromise the immediate planned uses of the major released volatiles, water and carbon dioxide, but does encourage the use of relatively low extraction temperatures to minimize release of S and N gases and simplify the processing scheme. At a later stage, when propellant production is underway, higher release temperatures and more complete gas extraction will be required: dealing with these impurities will then become essential.

In the context of the present research, our ultimate purpose in studying water extraction is to make available the raw materials for synthesizing storable chemical propellants. However, it is also obvious that water itself is a storable propellant that can be utilized by several different types of propulsion systems that derive their energy from sources other than chemical combustion.

There are several notional electrical propulsion schemes for using water as the working fluid, all at an early stage of development. All depend on the generation of large levels of electric power by means of photovoltaic arrays (or nuclear reactors). The principal alternative to electric propulsion is Solar Thermal Propulsion using water, in which a lightweight solar collector focuses sunlight onto a highly refractory rhenium thrust chamber and heats it to very high temperatures,

2800 to 3000 K. Water is then run into the thrust chamber where it flash-evaporates and exits from the thrust chamber nozzle as extremely hot water vapor. Specific adaptations of STP technologies can deliver specific impulses as high as 400 to 1100 s. STP is a very high thermal stress mechanism, so it is hard to design a spacecraft that uses it. Studies by James Shoji and coworkers, beginning at Rocketdyne in the 1960s under NASA and USAF funding¹², and recent work by teams at Ultramet, Marshall SFC, and UAH¹³ on fabrication of highly refractory rhenium thrust chambers, are valuable beginnings, but mission concepts for STP exist only on paper. A recent survey by Kennedy¹⁴ summarizes the prospects for STP use.

Solar Thermal Propulsion is singularly suited to moving massive bags of material (water, storable propellants, metals, radiation shielding, and raw materials) from one place to another. In addition to moving asteroid material to HEEO, there will be a need to move large amounts of mass from LEO to GEO, the Moon, or to Mars for exploration or settlement. At high propellant flow rates and chamber temperatures similar to that of a hydrogen-oxygen flame, the water exhaust can deliver close to 400 seconds I_{sp} . At very high temperatures of 2800 to 3000 K and at low water flow rates (low chamber pressures) water vapor extensively dissociates into H and O atoms, causing a decrease of the mean molecular weight of the exhaust from 18 to 6. The combined effect of the higher temperature and the lower molecular weight is to increase the specific impulse to over 600 seconds at the sacrifice of high thrust levels. The ability of rhenium to resist oxidative attack by water vapor under these extreme conditions is problematic, suggesting consideration of thoria (ThO_2) as the thrust chamber material. The performance of such a propulsion system, whether using rhenium or thoria, should be relatively insensitive to the presence of trace impurities such as ammonia and sulfur dioxide.

A very important point is that a propulsion system that uses sunlight directly has about a factor-of-5 advantage over solar electric systems because of the low conversion efficiencies of the latter, irrespective of distance from the Sun.

4. Electrolysis of Water for STP or Direct Combustion

Water can be electrolyzed into oxygen and hydrogen, and then the hydrogen liquefied for use in STP engines, in place of water. This achieves partial dissociation of molecular hydrogen, producing an exhaust with mean molecular weights between 1 and 2, and realizing I_{sp} values of at least 1000 seconds. STP technology, whether based on water or hydrogen, is obviously worth pursuing with the clear goal of using it specifically for our stated purpose of moving large loads of material. Each kilogram of exhaust from a water-driven STP engine contains nine times the mass and one third the velocity of the exhaust from a hydrogen STP engine operating at the same temperature, therefore delivering three times as much momentum as the hydrogen-driven

alternative. However, it is water we would be mining, not hydrogen: the amount of exhaust momentum (total impulse) per kilogram of mined water for the water exhaust system is 27 times as high as for the hydrogen exhaust system. Clearly, grasping for the highest possible I_{sp} is the wrong strategy: maximum total impulse from our mined water is what we require. This does not rule out the use of hydrogen-exhaust STP systems for specialty applications, but does emphasize that the better performer, and also by far the simpler of the two alternatives for moving large masses, is direct use of water as the exhaust.

Electrolysis of water and burning of the gases can provide 300 to about 380 seconds I_{sp} . This technique can be implemented either by electrolysis of water and refrigeration/liquefaction of hydrogen and oxygen on the asteroid, or by real-time combustion of the electrolysis products in flight. Again, the most difficult part is in designing an electrolysis and refrigeration/liquefaction system that produces cryogenic liquid oxygen and hydrogen. The technology of H/O thrusters is of course well understood, so long as the propellant enters the thruster as cryogenic liquids.

Mason Peck's version of this scheme¹⁵ (with the evolved gaseous H_2 and O_2 from electrolysis going directly into the combustion chamber), which can roughly be characterized as "storable" in the sense that it is non-cryogenic, probably has a slightly lower I_{sp} than the cryogenic version, but promises lower overall mass and greater reliability through simplicity for the engine and propellant-handling system because cryogenics are avoided. The problem with this "prompt use" scheme arises from the need to do large-impulse burns, such as for Earth capture, quickly: this requires accumulating a large mass of gaseous hydrogen and oxygen, which while avoiding the penalties associated with liquefaction and refrigeration, incurs a compensating penalty because of the large tank volumes and masses needed to contain the gases until their use.

The closely related HYDROS¹⁶ thruster from Tethers Unlimited is a pulsed gaseous $O_2 + H_2$ thruster with a very low level of complexity and an I_{sp} of about 300 s. It is possible to make a rocket out of this mechanism, but difficult to make a good one. In any case, avoidance of cryogenics is a great simplifying factor; however, here again the requirement for storage of large masses of gas to make short, high-impulse burns implies high tank volumes and pressures and thus incurs countervailing tankage penalties.

The use of gaseous hydrogen and oxygen also implies that cryogenic liquids are not available for regenerative cooling of the thrust chamber. We envision the use of water for any required cooling of such engines. Obviously care should be taken to minimize the sulfuric acid content of the coolant stream.

5. Electrolysis of Water for Manufacture of Storables

Production of fuels and oxidizer from asteroidal feedstocks requires the use of water and carbon oxides to manufacture combustible organic fuels and hydrogen peroxide oxidizer. The manufacture of fuels inevitably requires the use of hydrogen and carbon oxides; the production of H_2O_2 requires the use of water and oxygen. Production of the necessary hydrogen and oxygen gases is by means of electrolysis of water. Since water itself is a poor electrical conductor, low concentrations of electrolytes such as salts, ammonia, sulfuric acid, or alkali metal hydroxides must be present in the water, a condition that is likely to be met automatically in water condensed from a CI or CM source. Hydrogen is released at the cathode and oxygen is released at the anode. In terrestrial applications, gravity naturally separates the evolved gases from the liquid electrolysis medium; in space, as on the ISS¹⁷, where electrolysis of water is used to regenerate oxygen for breathing, the equipment design incorporates a method of separating gases from liquid and keeping the evolved gases separate from each other to avoid producing explosive mixtures. This is a mature high-TRL technology with years of flight heritage.

The energy (enthalpy) cost of liquid water electrolysis is 286 kJ per mole (15.9 GJ/tonne) of water, which must be supplied by photovoltaics. (Note that electrolysis of water is more energy-intensive than extracting the water from its host minerals.) We shall first consider a system architecture in which electrolysis of water takes place on an asteroid. A typical asteroid with a useful (volatile-rich) composition and an accessible orbit (low i ; q close to 1 AU) may have aphelion distance Q between 2.5 and 3.3 AU; for the moment, we shall use 3.16 AU for purposes of illustration (although obviously lower aphelion distances would be preferable). The intensity of sunlight at aphelion then would, as above, be 10% of the Solar Constant at 1 AU, or a thermal flux of $135 W_t/m^2$. Assuming 20% conversion efficiency for sunlight into bus power, we can expect $27 W_e/m^2$ of solar array area. At these large distances from the Sun, it is highly desirable to save weight by using a large, light-weight reflector to concentrate sunlight onto a much smaller area of solar cells: a 10:1 concentration ratio and a collection efficiency of 85% permits 1 MW_e electrical power generation at 3.16 AU by collecting 6 MW_t of sunlight, which requires a collector area of $4 \times 10^4 m^2$, a circular reflector with a diameter of 226 m. The photovoltaic array would then cover $3700 m^2$, a 61 m square. Over one year, this system at 3.16 AU could electrolyze 1875 tonnes of water, or about a half tonne per square meter of photovoltaic cells. However, the requirement to spend one entire year on propellant synthesis may be a serious detriment to the economics of the mission, forcing the use of non-optimum launch windows for both the outbound and inbound legs.

During the processing of water, there is also a possibility of electrolyzing water vapor by means of solid-state electrolysis, using yttrium-doped zirconia membranes. This technology is virtually identical to that developed for use in high-temperature gas-phase electrolysis of carbon dioxide into CO and oxygen for use in propellant production on Mars. Conduction of the O_2^- ion through the membrane permits separation of oxygen from hydrogen. The gas-phase electrolysis of water vapor also requires less electrical power than liquid-phase electrolysis of water, since the vapor

already has a substantial heat content. Although the total energy cost of production of hydrogen and oxygen is unchanged, electrolysis of the vapor leads to a more favorable (lower) ratio of electrical to thermal energy demand, which reduces the mass and complexity of the electrical power generation equipment. This advantage is lost if the heating is provided electrically.

At 1 AU from the Sun, the preferred location of the propellant manufacturing and storage facility, the solar flux is 10 times as large and the area and mass of all solar collectors and photovoltaic arrays are 10 times smaller than those that would have been required at the asteroid's aphelion. Further, the time available for processing becomes both longer and more flexible. In, for example, highly eccentric Earth orbit (HEEO) or an Earth-Moon Lagrange point, a 5 MW_t solar collector would require a diameter of only 70 m.

6. Where Should we Make Propellants?

To attempt the manufacture of storable propellants on a pioneering asteroid-mining mission is to depend on a complex mechanical and chemical system operating on an imperfectly characterized feedstock in a hostile environment in which we have little relevant experience. The task of carrying out an early synthesis and retrieval of propellants should not be entrusted to such a complex autonomous system. We strongly favor the use of the first retrieval mission to extract sufficient impure water for use of a Solar Thermal Propulsion system to return 100 tonnes of water (and a sample of unprocessed asteroidal material) to Earth orbit, where experiments to optimize the processing scheme for that exact composition type can be carried out. After the first retrieval mission, we envision massive extraction of impure water and CO₂ at the asteroid, which enables the use of solar thermal propulsion to return hundreds of tonnes of these materials to the Earth-Moon system. It is more realistic to imagine the processing steps that manufacture propellants as occurring at 1 AU from the Sun, in Earth orbit, under direct human supervision or via teleoperation. The propellants thus produced would then be available close to the site of their greatest demand, in LEO, GTO, GEO, and HEEO (for crewed missions to Mars, because assembly and final fueling in HEEO has some advantages over marshalling the units in LEO).

7. Storage and Transportation of Water and Carbon Dioxide

Carbon dioxide readily forms a clathrate hydrate under easily accessible conditions. At elevated CO₂ pressures (about 30 bars) the solid hydrate even forms spontaneously¹⁸ from liquid water at temperatures up to 281 K. At 10 bar pressure, liquid carbon dioxide and water ice form a solid hydrate of approximate formula CO₂5.75 H₂O that is stable between 230 and 273 K, and at 1 bar pressure the hydrate is stable from 192 to 218 K (Fig. 4), close to typical NEA surface temperatures. It is useful to note that the clathrate hydrate, once formed, is resistant to gaseous CO₂ loss even outside its equilibrium stability range: when solid clathrate hydrate is heated to 240

K (22 K above the phase stability boundary in Fig. 4) at 1 bar pressure, only 3% loss of gas occurs¹⁸. With further heating at 1 bar, the hydrate persists metastably up to 271 K, at which temperature it decomposes rapidly.

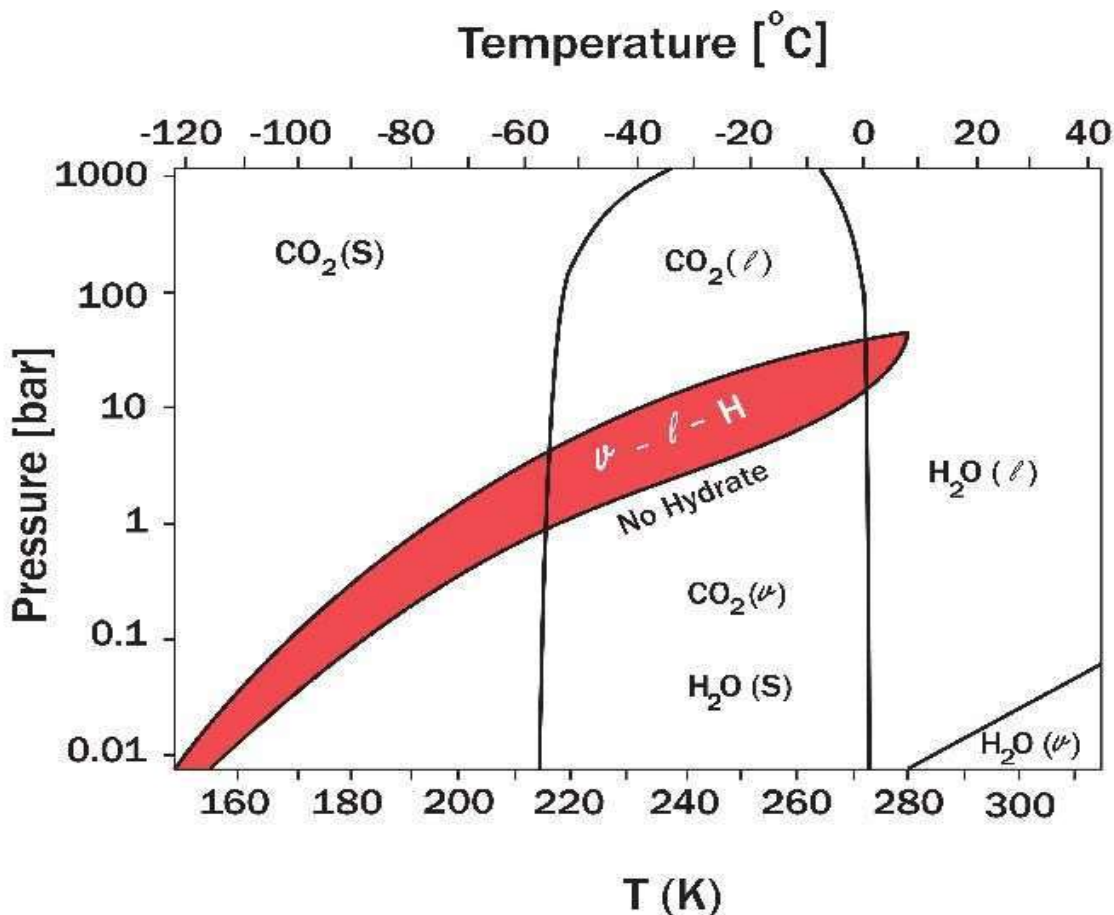


Fig. 4 The equilibrium stability field of CO₂ clathrate hydrate (H; the red-shaded area) vs. pressure and temperature. At temperatures below the lower stability of the hydrate water ice coexists stably with liquid or solid CO₂; at temperatures above the stability field, there is insufficient CO₂ pressure to force formation of the hydrate. However, the hydrate, once formed, has a high activation energy barrier for loss of CO₂ and can persist metastably up to about 271 K at 1 bar pressure.

The observed metastable persistence of the hydrate outside its equilibrium stability field is due to the high activation energy for escape of carbon dioxide molecules from their clathration sites.

Alternatively, cooling the hydrate from formation conditions within the equilibrium stability field and storing the hydrate at lower pressures is even less risky because the lower temperatures inhibit the, diffusion of CO₂ molecules out of the clathrate lattice even more strongly.

gases make a single pass through a two-layer catalyst bed, appears to hold much more promise because of its simplicity and efficiency²⁰. That direct synthesis from CO and H₂ is most efficient in the presence of methanol. Methanol production requires lower pressures than DME production, and may be preferable despite its somewhat inferior performance as a propellant (lower I_{sp}).

Kinetic modelling of the synthesis of dimethyl ether in a single reaction step²¹ from (H₂ + CO) and from (H₂ + CO₂) shows that the reaction of CO is faster and more efficient over a CuO–ZnO–Al₂O₃/γ-Al₂O₃ bifunctional layered catalyst, in which the first catalyst layer makes methanol and the second (γ-alumina) layer dehydrates methanol to DME. This model fits well the experimental results obtained in an isothermal fixed bed reactor over a wide range of operating conditions: 225–325 °C; 10–40 bar; space time, 1.6–57.0 (g of catalyst) h (mol H₂)⁻¹. The rate-limiting step is the synthesis of methanol from (H₂ + CO). Synthesis from (H₂ + CO₂) is much less important. Methanol dehydration by the γ-Al₂O₃ catalyst is very fast but requires high pressures. Water in the feedstock has an inhibiting effect on the synthesis of methanol and the formation of hydrocarbons. This single-step, two-catalyst process permits attainment of yields higher than 60% of carbon converted into DME and 5% into methanol, when (H₂ + CO) is fed at 30 bar and 275 °C. The unreacted gas is dried and recirculated through the reactor. Note that, at higher reactor temperatures, hydrocarbons (mainly methane) are produced.

If the feedstock is rich in carbon dioxide, a modification of this scheme is required. A study of another bifunctional catalyst system²² using CuO–ZnO–Al₂O₃–ZrO₂ plus HZSM zeolite (where the γ-Al₂O₃ catalyst is again responsible for conversion of methanol into DME) was used for the conversion of a CO₂–H₂ mixture. Conversion efficiencies of CO₂ into DME reached 21% with a methanol yield of 5.9% when the reaction was run at 5 MPa and 523 K. They also found that, not surprisingly, recycling of the dried CO made in this process was desirable for improved efficiency.

Separation of the DME from the methanol and water is required and can be conducted using a molecular sieve process.

A large-scale commercial application of DME production via CO₂ recovery is underway in Iceland²³, where Mitsubishi has opened a plant for conversion of captured CO₂ into methanol and thence into DME in a two-stage process utilizing the same basic chemistry as the previous system. They process CO₂ emitted from a ferrosilicon plant, scrubbing the flue gases to remove sulfur as sulfuric acid in order to protect the catalyst bed. The source of hydrogen gas is electrolysis of water. Again, the last step in the process is making DME via the dehydration of methanol using a γ-Al₂O₃ catalyst.

DME is the more desirable product because it has a higher heat of combustion (both per mol and per gram) than methanol and, unlike methane, is not a cryogen. There are distinct advantages to storing DME at local (asteroidal) ambient temperatures (-20 to -60 °C) because its normal boiling

point is $-24.81\text{ }^{\circ}\text{C}$ and the vapor pressure of DME at $0\text{ }^{\circ}\text{C}$ is 5 atm^{24} . The vapor pressure equation calculated from measured temperature points down to $-25\text{ }^{\circ}\text{C}$ is given by $\log_{10} p_v(\text{DME}) = 7.69056 - 1909.75/T(\text{K})$, with pressures in atmospheres. At $-50\text{ }^{\circ}\text{C}$ the vapor pressure is only 0.135 atm . DME's freezing point of $-138\text{ }^{\circ}\text{C}$ (135 K) is so low that maintaining DME as a liquid would not be difficult. The freezing point of methanol is 40 degrees higher.

All that is lacking is a storable oxidizer that can be co-produced from the same reactants (water, carbon oxides) as DME: we propose hydrogen peroxide.

9. Conventional (Earthsideside) H_2O_2 Synthesis

Commercial hydrogen peroxide synthesis generally uses the anthraquinone process, which is dependent on an organic catalyst that has limited lifetime and cannot be replenished from sources in space. A conceptually appealing alternative, direct synthesis of H_2O_2 from H_2 and O_2 , is a relatively new process that is not without problems of its own, but which is under active development²⁵. Interestingly, recent research has shown the advantage of carrying out the direct synthesis of hydrogen peroxide in a methanol medium²⁶.

Very recent research shows that using a palladium catalyst in an acidic medium^{26b} in which the acid functional groups or halogens are bound to a catalyst bed such as sulphated zirconia, or using a Pd-Au catalyst, improves the efficiency of hydrogen peroxide direct synthesis. Recent research has focused on the adaptation of this system to a continuous-flow rather than a batch reactor. A selectivity of 90% has been demonstrated with such a continuous reactor^{26c}: as much as 90% of the reactant flux emerges as H_2O_2 , and 10% as water. Higher concentrations of H_2O_2 would require low-temperature distillation to remove unwanted water, or the solution could be used exactly as produced. The hazard of using a hydrogen/oxygen gas mixture was avoided by using a large amount (80%) of carbon dioxide as the carrier gas. As sanguine as the abstract of their article is, the text is more sobering, in that the observed selectivity declines with time after a brief startup interval. This scheme must be regarded as being in the preliminary research stage, definitely not ready for use in a production plant. Its suitability for space-based application is not yet demonstrated.

Edwards, et al.^{26d} of the University of Cardiff have found that directly synthesized H_2O_2 can be stabilized against further hydrogenation (reduction to H_2O) driven by the very same catalysts used in the H_2O_2 synthesis. Their technique is a simple acid pretreatment of the carbon support for the gold-palladium nanoparticle catalyst. This treatment blocks the sites of the reduction reactions, giving high selectivity for peroxide synthesis.

10. Space-based direct synthesis of H₂O₂

H₂O₂ synthesis from H₂ and O₂, which is required for space-based storable oxidizer production, is a new alternative to existing terrestrial practice for production of hydrogen peroxide. Advances made in the pursuit of space-based direct synthesis will feed back into terrestrial H₂O₂ production, potentially accelerating the replacement of chlorine-based oxidizing and bleaching agents. Of the many suggested processes for direct synthesis of hydrogen peroxide, the one that appears most promising for space-based use is an electrochemical cell.

Recent fuel-cell research has been inspired by the automobile industry's efforts to develop fuel-cell powered vehicles as replacements for internal combustion engines. Fuel cells oxidize a fuel such as hydrogen or hydrocarbons under controlled conditions to generate an electric current without the undesirable byproducts of normal combustion, such as partially oxygenated unburned hydrocarbons (aldehydes, ketones, carboxylic acids) and nitrogen oxides.

The ideal fuel for fuel cell use is hydrogen. The end product of the power fuel cell reaction is water. However, the reactions in the fuel cell proceed in two stages: the first stage produces hydrogen peroxide, and the second converts all the H₂O₂ to water. For road vehicles, there is a strong incentive to maximize energy output by avoiding formation of H₂O₂. However, the same fuel cell technology could also be optimized for H₂O₂ production. Research on this alternative is at an early stage. Professor David Schiffrin, director of Liverpool University's Center for Nanoscale Science, undertook an investigation of optimizing hydrogen peroxide production, initially using quinones rather than platinum catalysts. Schiffrin and his colleagues have a patent pending for co-generation of electricity and hydrogen peroxide²⁷. Their experiments to date on electrode development have been very successful, but no attempt has been made to adapt these electrodes to a complete H₂O₂ production cell, let alone for space applications. For use in space, it would also be desirable to avoid dependence on degradable catalysts (such as anthraquinone) that would require resupply from Earth. Schiffrin's patent application specified the use of a platinum-group metal for the hydrogen oxidation electrode and "oxides of cobalt alloys", carbon with attached anthraquinone derivatives, or "transition metal complexes (e. g. cobalt porphyrin), gold, copper, mercury, or platinum" for the oxygen-reduction electrode. As a side benefit, electricity produced by the process permits the chemical potential energy change of the cell reaction to benefit both hydrogen peroxide synthesis and energy production, thus recapturing part of the energy expended in making hydrogen and oxygen by water electrolysis. This technology, although very promising as a route to efficient synthesis of H₂O₂, is still in the early stages of development and needs to be adapted to use in space, an important goal for Phase II.

Their success to date does however give grounds for optimism that a simple and capable system may be attainable. Unfortunately, Prof. Schiffrin is now retired and no longer maintains a laboratory. Experimental facilities at the University of Arizona can continue this research.

11. Long-Term Storage of Hydrogen Peroxide

Decomposition of H_2O_2 : Hydrogen peroxide spontaneously decomposes into water and oxygen with substantial release of heat, a trait that makes it valuable as a rocket monopropellant. Its structure, HO-OH, is analogous to that of hydrazine, $\text{H}_2\text{N-NH}_2$, an even more powerful monopropellant that is much harder to make in space because of the low availability of nitrogen.

The heat released upon decomposition of hydrogen peroxide at 298 °C is -98.21 kJ/mol. The rate of decomposition of high-test peroxide (HTP; a name usually reserved for solutions with 90% purity or higher) depends on temperature, exposure to light, catalytic impurities, and exposure to some solid surfaces.

Storage container materials: Many plastics and certain stainless steel alloys are useful containers for long-term storage of HTP. One favored tank material for hydrogen peroxide storage is 1060 aluminum alloy. Teflon or Teflon-coated tanks are also very successful.

Light: Hydrogen peroxide is vulnerable to destruction by near UV in sunlight, and is for this reason stored in opaque containers. Food-grade (35%), hair bleach (6%) and drugstore (3%) H_2O_2 are sold in opaque containers or brown bottles to inhibit destruction by light.

Base- and metal-catalyzed decomposition of H_2O_2 : Alkaline solutions of H_2O_2 are degraded by exposure to hydroxide ion. Strong acids are also detrimental; much practical experience shows that the optimum pH for H_2O_2 storage is about 6 (weakly acidic). A wide variety of metal cations, including Ca^{2+} , Mg^{2+} , Al^{3+} , and transition metal ions, also catalytically destroy H_2O_2 . Since the favored tank material is an aluminum alloy, it is essential to regulate the pH of the solution so as to minimize the dissolution of Al, not only to protect the tank from excessive corrosion and eventual failure, but also to protect the H_2O_2 in it from catalytic decomposition. This requirement also mandates a near-neutral pH, since Al metal is dissolved in both strongly acidic (as Al^{3+}) and strongly basic (as $\text{Al}(\text{OH})_4^-$) solutions. Catalytic degradation can be prevented by assuring that the peroxide stream is free of particulates, dissolved metals and sulfuric acid.

Temperature: Elevated temperatures accelerate the decomposition of H_2O_2 in any tank material. High-concentration H_2O_2 , of 90 to 99% purity, with stannate stabilizer added (see below), has been stored successfully for many years in 1040 Al-alloy tanks, showing decomposition rates²⁸ of about 0.01%/year at 86°F (303 K), 0.1%/year at 151°F (339 K), and 1%/year at 212°F (373 K). These measured rates define the activation energy for decomposition, which permits a calculation of the decomposition rate at lower temperatures such as might be applicable in a space environment. Fig. 5 shows that decomposition rates of 0.001%/year can be achieved at a temperature of about 37°F (3°C).

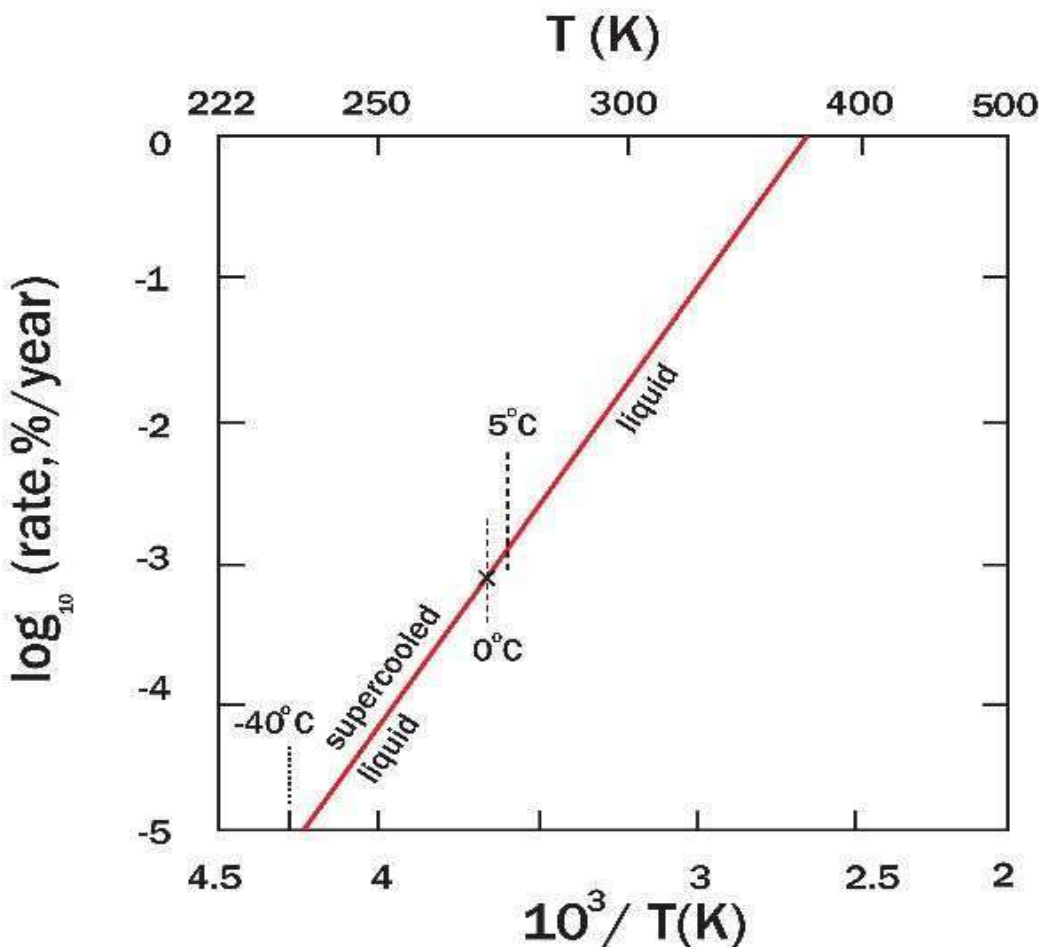


Fig. 5 Rate of decomposition of HTP H₂O₂ in Al-alloy tanks. Experimental data above 300 K are used to calculate the activation energy for decomposition and extend the curve to lower temperatures. The normal freezing point of HTP is -0.4 °C; however, because of the tendency for liquid H₂O₂ to supercool, the liquid can persist down to about -40 °C, allowing the prediction that the actual H₂O₂ decomposition rate for the supercooled liquid may be as low as 10⁻⁵ %/year at 233 K. See Fig. 6 for context.

A one-tonne tank load of high-purity H₂O₂ at 0 °C would then lose about 10 g of material per year, releasing about 5 g of oxygen gas. Likewise, 100 tonnes of HTP at -40 °C would lose about the same amount of oxygen. There seems to be little data on how much solid H₂O₂ gains in stability relative to the liquid: the freezing point of pure H₂O₂ is -0.4°C (31°F). There is, however, a patent (U. S. Patent 3,480,557) on storage of H₂O₂ in the solid state using complex organic substrates, a technique unlikely to be of interest in space.

Stannate preservative: Addition of sodium or potassium stannate (Na,K)₂Sn(OH)₆ has a strong stabilizing effect on H₂O₂, in part by reacting with, complexing, and even precipitating metal stannates from solution and making them unavailable to react with H₂O₂. US Patent 3383174A²⁹ is illustrative of one of many variants on the use of stannates at concentration levels of 0.001 to 0.01% to stabilize high-purity peroxide. The purpose of the higher concentrations is to protect

stored high-test peroxide against the effects of catalytic decomposition catalyzed by trace metal ions in the water used to dilute the peroxide for practical use, a factor absent in our proposed use. The mass of stannate required to stabilize 100 tonnes of 98% H_2O_2 destined for propellant use (not for dilution) is therefore on the order of 1 kg.

Phosphates also find commercial use as stabilizers for peroxide.

12. Effect of Peroxide Degradation on Propellant Performance

Calculations performed on burning kerosene (jet fuel) with 98% H_2O_2 at 50 atmospheres chamber pressure show an I_{sp} of 329 seconds²⁸. Using hydrogen peroxide stored for about 2 years³⁰, after the concentration had dropped to 96%, the computed specific impulse was found to have dropped only about 0.6%, to 327 s. The reason that the drop in performance was so small is that the small amount of additional water vapor made by H_2O_2 decomposition has a lower molecular weight than carbon dioxide, leading to an exhaust with a lower mean molecular weight and higher thermal velocity at any temperature. The lowering of the molecular weight of the exhaust partially compensates for the lower oxygen content. Thus slight (2%) degradation of the concentration of the oxidizer has only a very small (0.6%) effect on engine performance.

13. Freezing and Distillation Behavior of Hydrogen Peroxide

As mentioned above, the freezing temperature of pure hydrogen peroxide is $-0.4\text{ }^\circ\text{C}$, very similar to that of pure water. The $\text{H}_2\text{O}_2/\text{H}_2\text{O}$ binary phase diagram shows a eutectic point at about $-54\text{ }^\circ\text{C}$ and 64% hydrogen peroxide, a concentration so low that serious performance degradation is incurred. A representation of the $\text{H}_2\text{O}_2/\text{H}_2\text{O}$ equilibrium phase diagram on the $p\text{H}_2\text{O}_2$ - $p\text{H}_2\text{O}$ plane is given in Fig. 6. Each freezing-point line in the figure is the locus of coexistence between two phases, the liquid and the locally stable solid. Cusps in the liquidus correspond to triple points in the $\text{H}_2\text{O}-\text{H}_2\text{O}^2$ system.

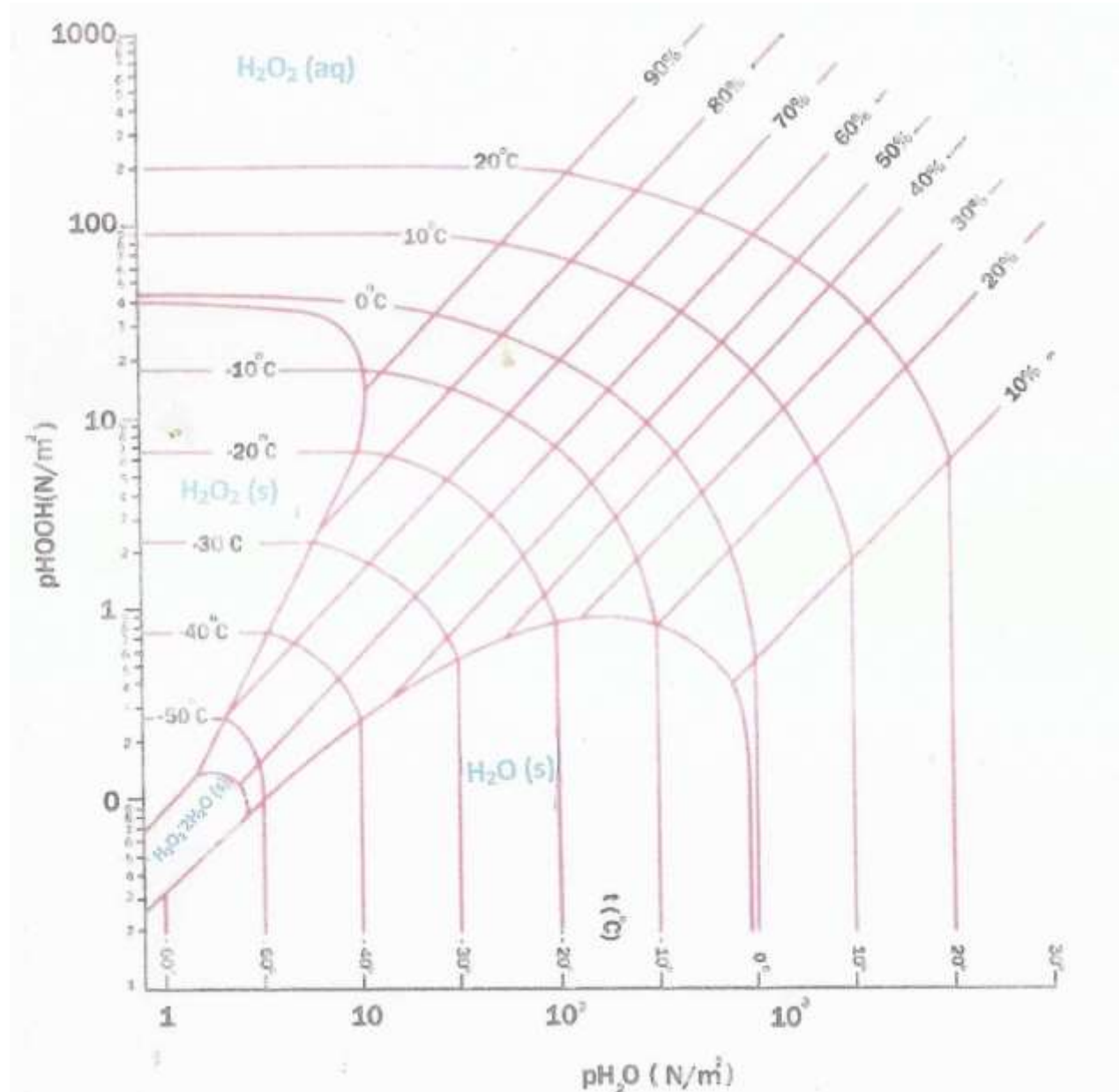


Fig. 6 Equilibrium phase diagram of the H₂O₂-H₂O system on the $p(\text{H}_2\text{O}_2)$ - $p(\text{H}_2\text{O})$ plane. The solid scalloped line is the freezing-point curve for aqueous H₂O₂ solutions; the upper right region of the diagram, that above the freezing point curve, is the solution stability field, within which (curved) lines of constant temperature (isotherms) and (straight) lines of equal solution concentration (isopleths) are shown. The region below the freezing curve on the left side of the diagram is the stability field of pure solid H₂O₂; the region below the freezing curve at the bottom of the diagram is the stability field of water ice Ih. A solid hydrate of hydrogen peroxide is stable in the small region at the lower left. See text for further interpretation.

The diagram shows that a 60% solution at 0 °C has a hydrogen peroxide partial pressure of 10 N/m^2 and a water vapor partial pressure of 180 N/m^2 , so the vapor has a water:peroxide ratio of

18:1, far higher than the ratio in the liquid (0.4:0.6, or 0.66). Thus removal of vapor (distillation) increases the concentration of H₂O₂ in the liquid. Low-temperature (vacuum) distillation of the solution therefore provides a straightforward way to evolve the liquid toward pure-H₂O₂ composition. Alternatively, given a low level of artificial gravity (acceleration) it may also be desirable to take advantage of the two-phase region to freeze out pure H₂O₂ and separate it from residual liquid via flotation or filtration.

Freezing of hydrogen peroxide, however, is dependent upon the presence of suitable nucleation sites, in the absence of which the liquid high-test peroxide (HTP) can be severely supercooled³¹, often remaining as a liquid down to -40 °C. Thus pure peroxide, once made, can be stored as a liquid even far below its normal freezing point, at temperatures similar to the ambient temperatures on the surfaces of Near-Earth Asteroids, without incurring the handling complexities caused by freezing into an icy solid. A further benefit is that the lower the storage temperature, the slower the rate of hydrogen peroxide decomposition. By reference to Fig. 5, we see that extension of the decomposition rate curve into the supercooled liquid region (under the assumption of a constant enthalpy of activation) predicts that the rate of decomposition of liquid HTP at -40 °C is only 10⁻⁵ %/year, fully 100 times slower than the rate at the normal freezing temperature.

14. Raw Materials Requirements for Storable Propellant Synthesis

The overall stoichiometry of synthesis of DME and H₂O₂ from H₂O and CO₂ is:



The 9:2 molar ratio of water to carbon dioxide implies a mass ratio of $(9 \times 18)/(2 \times 44) = 1.84$ tonnes of water per tonne of CO₂; synthesis of 1000 tonnes of propellant requires 648 tonnes of water and 352 tonnes of CO₂.

There is a stable and easily produced solid hydrate of carbon dioxide, water clathrate hydrate, that serves as a means of transporting both CO₂ and water (see Fig. 4). The hydrate provides 5.75 water molecules per carbon dioxide molecule, somewhat more than the stoichiometric ratio of 4.5:1 desired for propellant synthesis:



Return of sufficient hydrate materials to make 1000 tonnes of propellant would require carrying an extra 141 tonnes of water beyond the 648 tonnes calculated above for propellant synthesis, necessitating a total mass return of 1141 tonnes. The 141 tonnes of “extra” water can be used in any of a wide variety of ways, such as in life support, hydroponics, as an industrial reagent, and in electrolytic manufacture of LOX and LH₂. To this total should be added the amount of water

needed by the propulsion system (water-based STP) to return the load to Earth orbit. That amount is highly mission-dependent, and must be stored separately from the clathrate.

Since water release is efficient at relative low calcining temperatures, and efficient CO₂ release requires temperatures so high that SO₂ is also produced abundantly, there is a strong incentive to seek propellant production schemes that use a high ratio of water to CO₂. The following table illustrates the availability of fuel/oxidizer pairs vs. the mole fraction of CO₂ in the retrieved payload of asteroidal volatiles.

Table 1. Potential fuel/oxidizer pairs compared to feedstock composition

	Fuel	Oxidizer	Production reaction	Mole fraction CO ₂
A	H ₂	O ₂	2H ₂ O → 2H ₂ + O ₂	0
STP	(H ₂ O STP)		H ₂ O	0
B	H ₂ O ₂ mono		2H ₂ O → H ₂ O ₂ + H ₂	0
C	CH ₄	H ₂ O ₂	CO ₂ + 6H ₂ O → CH ₄ + 4H ₂ O ₂	0.143
	feedstock		CO₂ + 5.75 H₂O → CO₂ 5.75H₂O	0.148
D	CH ₃ OH	H ₂ O ₂	CO ₂ + 5H ₂ O → CH ₃ OH + 3H ₂ O ₂	0.167
E	C ₂ H ₆	H ₂ O ₂	2CO ₂ + 10H ₂ O → C ₂ H ₆ + 7H ₂ O ₂	0.167
F	DME	H ₂ O ₂	2 CO ₂ + 9H ₂ O → (CH ₃) ₂ O + 6H ₂ O ₂	0.182
G	C ₂ H ₅ OH	H ₂ O ₂	2 CO ₂ + 9H ₂ O → C ₂ H ₅ OH + 6H ₂ O ₂	0.182
H	C ₃ H ₈	H ₂ O ₂	3CO ₂ + 8H ₂ O → C ₃ H ₈ + 4H ₂ O ₂	0.273
I	CH ₄	O ₂	CO ₂ + 2H ₂ O → CH ₄ + 2O ₂	0.333
J	CH ₃ OH	O ₂	2CO ₂ + 4H ₂ O → 2CH ₃ OH + 3O ₂	0.333
K	DME	O ₂	2 CO ₂ + 3H ₂ O → (CH ₃) ₂ O + 3O ₂	0.400
L	C ₂ H ₆	O ₂	4CO ₂ + 6H ₂ O → 2C ₂ H ₆ + 7O ₂	0.400
M	C ₂ H ₅ OH	O ₂	2CO ₂ + 3H ₂ O → C ₂ H ₅ OH + 3O ₂	0.400
N	C ₃ H ₈	O ₂	3CO ₂ + 4H ₂ O → C ₃ H ₈ + 5O ₂	0.429

It is evident from this table that there are five propellant-production schemes (C, D, E F and G) that have feedstock compositions that match that of the clathrate hydrate reasonably well, all of which involve the use of hydrogen peroxide as the oxidizer. Of these, option C employs cryogenic methane (normal boiling point 112 K) and E involves the mild cryogen ethane (b. p. 184 K). The storable fuel options are reduced to methanol and DME.

Options A, STP and B do not depend on CO₂ at all. Options A and B employ water and solar electrical power (for electrolysis); STP employs water and concentrated direct solar heating. Assuming conversion of raw solar power into electricity with an efficiency of 25%, B is preferable to A for most purposes when carbon is not available. The carbon-intensive fuels near the bottom of the list (I through N) are especially poor choices for manufacture from C asteroid volatiles: all also demand cryogenic LOX.

15. DME/H₂O₂ Combustion

Since the combustion of DME with hydrogen peroxide produces only carbon dioxide and water vapor as products, the stoichiometry of the combustion reaction is exactly the same as the synthesis reaction, requiring 6 moles of H₂O₂ per mole of DME burned. The exhaust then has a mean molecular weight M of 22.7, compared to 30 to 31 for the combustion products from burning a long-chain hydrocarbon (kerosene) with LOX. The high H:C ratio in the combustion products guarantees a lower exhaust molecular weight, which in turn guarantees a higher mean thermal speed for any temperature. The H:C ratio in the DME fuel is 3:1 compared to 2.1±0.1:1 for long-chain hydrocarbons (kerosene; paraffin) and 1.9 for diesel fuel. The only fuels with a higher H:C ratio are the deep cryogen liquid hydrogen (∞) and the soft cryogen methane (4:1). Methanol (4:1), although it has a favorable hydrogen content, has a poorer heat of combustion because it is already 50% by mass oxygen – initial calculations indicate however that this deficiency is compensated by being closer to the feedstock ratio than DME (see previous section). This is examined further in Section 17. Ethane C₂H₆ (a soft cryogen) and ethanol CH₃CH₂OH also have H:C = 3:1, the same as DME.

The heats of combustion of these materials (ΔH_c) can be compared in the following table, which assumes the use of cryogenic LOX as the oxidizer for every fuel except DME and ethanol, for which high-grade hydrogen peroxide is assumed. All numbers assume a stoichiometric fuel:oxidizer ratio. The following table also gives the mean molecular weight M of the exhaust and a crude performance Figure of Merit (FoM) estimated from the ΔH_c and molecular weight, based on $I_{sp} \sim v_{ex} \sim (\Delta H_c/M)^{0.5}$. I_{sp} numbers from a variety of published sources are included in the rightmost column. Note that this FoM refers ONLY to performance as a propellant.

Table 2. Heats of combustion for assorted fuel/oxidizer pairs

Fuel	Oxidizer	Heat of Combustion (HHV) ³² (GJ/tonne)	Molecular Weight of Exhaust, AMU	FoM	I_{sp} (sec)
Liquid Hydrogen	LOX	134.0	18.0	2.81	390
Liquid Methane	LOX	52.4	26.7	1.44	362
Liquid Ethane	LOX	49.2	28.4	1.35	310
Gasoline	LOX	47.0 ³³	30.2	1.25	335
Kerosene	LOX	46.2 ³³	30.4	1.23	358
Diesel Fuel	LOX	45.0 ³³	30.6	1.21	300
Methanol	LOX	22.0	26.7	0.92	280?
Dimethyl Ether (DME)	HTP	43.8	22.7	1.18	300 (NOTE 1)
Ethanol	HTP	42.2	22.7	1.14	290
Methanol	HTP	31.9	22.3	1.20	261
Ethylene	HTP	70.5	23.2	1.74	?

NOTES:

1. DME/HTP I_{sp} predicted to be just higher than for Ethanol/HTP.

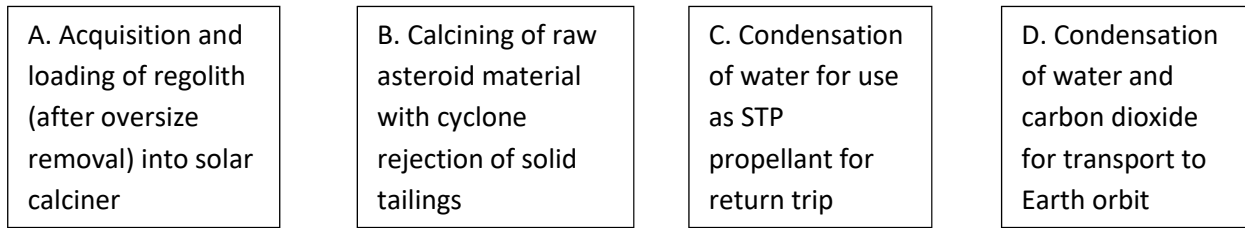
This table suggests that DME/H₂O₂ is reasonably competitive with most hydrocarbon/LOX systems. If mild cryogenics are considered, then methane or ethane with hydrogen peroxide would also be attractive options. All H₂O₂ combinations are somewhat inferior to methane/LOX in performance; their advantage is that they are cryogen-free.

16. Schematic Processing System Architecture on an Asteroid

The first mass-retrieval mission should be devoted to relatively low-temperature extraction of water for the STP system for the return of CO₂ hydrate and a mass of raw (unheated) asteroidal material to a processing facility in Earth orbit. (Confirming the feasibility of combined water and CO₂ harvesting on the first missions is a critical goal of the Phase II research.) The equipment that must be present on the asteroid includes a large solar collector to provide thermal energy for baking the asteroid material to release water-rich volatiles. Separation of the volatiles from residual solids can be accomplished efficiently by the same means widely used on Earth, a “cyclone” unit that spins the mixture to centrifuge the dust out of the gas and a “dust pump” to draw off the exhausted solids, which should be bagged and left on the asteroid for future exploitation for their content of residual volatiles and metals. The raw material returned to Earth orbit will be used to optimize the heating and processing techniques for future use on the asteroid.

For all later missions, stronger heating (following time/temperature parameters determined from experiments carried out in Earth orbit on the asteroidal solids returned in the first mission) will be used to drive off a larger mass of gas. This evolved gas, composed mainly of carbon dioxide and water vapor, is cooled to condense these materials as the carbon dioxide clathrate hydrate for return to near-Earth space for final processing into propellants, leaving a residual incondensable gas of nitrogen, carbon monoxide, and probably sulfur dioxide to be vented overboard. Supplemental liquid water is condensed into a separate tank for use as the working fluid in a Solar Thermal Propulsion engine for the return to near-Earth space.

The electric power for the pumps, valves, and cyclone must be supplied by a small photovoltaic array sized by the need to deliver sufficient power at the aphelion of the asteroid, where most of this volatile-extraction processing must occur. An electrolysis unit, if required, would be conceptually patterned after the ISS system: it and the other pieces of equipment mentioned (and the ISS Sabatier reactor) function independent of gravity. It would, however, be desirable to design the system architecture so that electrolysis and all other forms of processing could be relegated to Earth orbit, not used on the asteroid. On the target asteroid, after landing, anchoring, and deployment of the solar collector:



Step A uses an electromagnetic regolith “pump” to deliver a stream of loose, fine regolith through an airlock into a calciner tube which runs the length of a trough in an elongated solar collector with approximately parabolic section. In Step B, the material is heated as it transits the length of the calciner trough and releases volatiles, the volatiles and tailings being separated by passage through a cyclone which expels dust into a reservoir and admits gaseous products, largely water vapor and carbon dioxide, through a heat exchanger (which preheats the solids entering Step A) into a storage volume or “water bag” which, in Step C, rejects the heat of condensation into space. Somewhat impure water is accumulated in the bag in step C for use as the working fluid in a Solar Thermal Propulsion system to return the payload to Earth orbit. Lower temperatures are used in step D to condense CO₂ clathrate hydrate into a separate “ice bag” for transport to Earth as the main payload. The first processing stage, on the asteroid, has been modeled in detail for us by Sam Spencer, a DSI collaborator, as follows. This model, one of several produced by Spencer, deals with the problem of sulfur dioxide release at higher calcining temperatures by the expedient of using only lower calcining temperatures, which limits CO₂ production as well as preventing massive release of SO₂. (An alternative architecture involving higher calciner temperatures, efficient CO₂ production, transport of both water and carbon dioxide to HEO, and SO₂ cleanup on the asteroid has also been studied. A decision between these options awaits laboratory testing in Phase II.)

A detailed flow chart for the on-asteroid operations, developed by DSI collaborator Sam Spencer, shows the complete plan. “Area 1” is the surface of the asteroid.

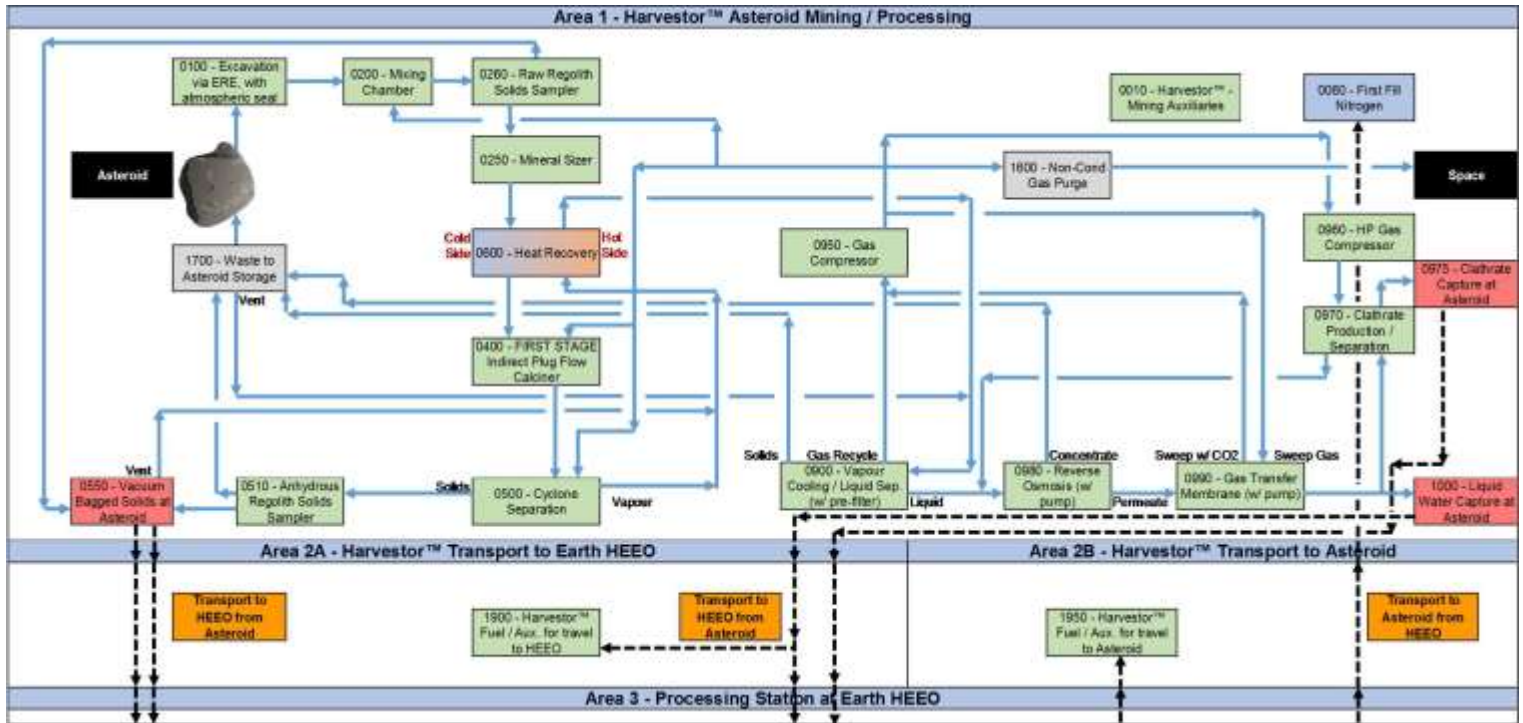


Fig. 7 Analysis of at-the-asteroid processing identified 13 major phases. The estimates for mass, power, and throughput will be greatly refined during Phase II work.

□ Area 1 – Asteroid Mining

○ Water supplied at HEEO:

- The basis for design is the supply of the maximum mass of water and CO₂ at HEEO – after transport, depending on the selected asteroid and return fuel requirements. Initial calculations indicate this may vary from 30 – 120 tonnes of water supplied to HEEO, constrained by the mass that can be launched to a target on a Falcon Heavy; however significant additional optimization is still to be conducted.

○ Material Handling:

- Asteroid particle size assumed to be as defined in literature of approximately d₅₀ = 50 μm, d₉₀ = 100 μm, d₁₀₀ = 10,000 μm. Anything larger than this will be rejected at the excavator stage.

○ Energy Production / Removal:

- Electrical energy supplied by solar photovoltaic cells with a solar cell efficiency of 25% and system efficiency of 80%
- Thermal energy supplied by Concentrated Solar Radiation via Parabolic Mirrors with a mirror efficiency of 60% and a system efficiency of 80%.

An additional efficiency of 75% is assumed for transfer of energy to final user.

- Energy removal is via ammonia coolant with radiative loss to space.
- Incident solar radiation is calculated at the furthest distance from the sun, and therefore varies from one target asteroid to another.
- Unit 0060 – First Fill Nitrogen:
 - A small amount of nitrogen (order of kg) will be bought from Earth for the purpose of pressurizing the system before use.
- Unit 0100 – Excavation:
 - Excavation using external Electromagnetic Regolith Extractors (ERE), with internal gas assistance for solid transfer as required.
- Unit 0200 – Mixing Chamber:
 - The solid:gas ratio for material transport is controlled to around 200-300. Experimental test work at zero gravity (by others) indicate that ratios up to 6000:1 are possible, however DSI would like to use a larger ratio to minimize risk of blockage.
 - A pressure of 50 kPa will be used for all processing sections, supplied via gas compressor and maintained by inert-gas recycling.
- Unit 0350 – Mineral Sizer:
 - This equipment will act as a safety device for the rest of the equipment, ensuring that oversize particles will be crushed and agglomerated material will be broken up. This equipment can be placed in any orientation, and will use pneumatic transfer to ensure transport through the sizer.
 - The operability of this equipment will need to be tested before use.
- Unit 0400 – Calciner:
 - Operating temperature of 1000K required to optimize CO₂ release at asteroid. Associated SO₂ release will be managed.
 - Residence time not yet defined, however due to small material size this is expected to measure in minutes – further testwork required.
- Unit 0500 – Cyclone Separation:
 - Cyclones work in zero gravity, so gas/solid separation should work well.
- Unit 0550 – Anhydrous Solids Capture:
 - Solids are captured and valuable gases removed before discharge back to asteroid. Gas losses, largely via adsorption, are expected at 1% w/w.
- Unit 0600 – Heat Recovery:
 - A simple heat exchanger (“recuperator”) will recover excess heat in the gases and heat the incoming solids.
- Unit 0900 – Vapor Cooling:

- The high level of water vapor in the gas ensures easier recovery of liquid water from cooling, using ammonia heat removal systems as previously discussed.
- Unit 0950 – Gas Compressor:
 - A simple gas compressor to provide pressure to the system.
- Unit 0980 – Reverse Osmosis or comparable technology:
 - Water treatment to remove any dissolved impurities from the water.
- Unit 0990 – Gas Transfer Membrane:
 - Further water treatment to remove a majority of the dissolved CO₂ from the water.
- Unit 1600 – Gas Purge:
 - A removal system for any additional non-condensable gases (N₂, CO, etc.) that build up in the system during operation. These gases are expected to be abundant enough to exceed makeup requirements for losses.

The next step is transport of CO₂ and water to a processing facility in HEEO. We have considered the option of returning some solid asteroid material (either heated or unheated) for process development research (such as metals extraction): “Area 2” refers to the transportation step.

- Area 2A – Transportation to Earth HEEO:
 - Thermal energy to heat water for use in Solar Thermal Propulsion (STP) as previously discussed. Mass of water and raw or anhydrous solids for experimentation are taken into account, along with all processing equipment.
- Area 2B – Transportation to Earth:
 - Heat water in a Solar Thermal Propulsion (STP) as previously discussed. Mass of first-fill N₂ taken into account, along with all processing equipment.

The task of manufacturing DME and HTP is relegated to a facility in Earth orbit to minimize the complexity of the autonomous equipment landed on the asteroid and to take advantage of the higher solar flux at 1 AU. Sulfur management would logically be done at the asteroid. This removal must precede the fuel production step to avoid poisoning the catalysts used in DME synthesis.

17. Schematic Processing System Architecture in Earth Orbit

The functions of the processing facility are to manufacture, store, and dispense propellant to all outbound missions, including return missions to the asteroids from which further extraction will be attempted, manned and unmanned missions to the Moon, and manned missions to the Mars

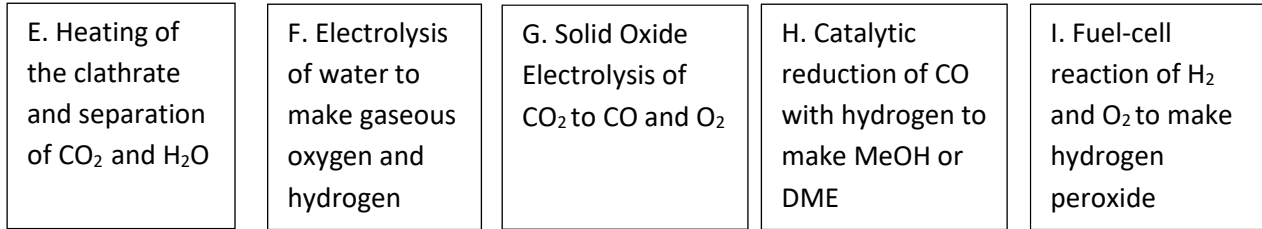
system. The orbital parameters of the facility must be compatible with access from an asteroid return vehicle newly arrived in the Earth-Moon system and to (and from) LEO, with perigee high enough to avoid prolonged exposure to van Allen Belt radiation. A Moon-resonant orbit would also be desirable. All these factors suggest Highly Eccentric Earth Orbit (HEEO) as the preferred location, in accord with the arguments presented many years ago by Benton C. Clark.

From the processing facility, an apogee burn can be used to drop the perigee of a departing spacecraft to as low an altitude as practical to take full advantage of executing escape burns deep in Earth's potential well (the Oberth effect). HEEO is also very desirable because it is close to escape velocity, and also because it facilitates dropping supplies into LEO or GTO via repeated mild aerobraking passes. Supplying storable propellants to LEO for station-keeping, attitude control, and reboost and for injection of outgoing payloads into GTO and GEO, or into rendezvous transfer orbits to the processing/refueling facility, are all potential major markets. The use of a HEEO with a Moon-resonant period permits integrating it into Moon-bound traffic flow, as well as facilitating lunar swingbys for outbound missions. Note that this is essentially an incarnation of NASA's plans for space-basing from the 1990 era. Great numbers of relevant NASA publications can be found by Googling NASA "space basing".

The fuel factory/depot would also become the logical place for production of cryogenic propellants as demand arises. Cryogenics are outside the scope of this work.

The feedstock for the propellant manufacturing scheme is CO₂ clathrate (or condensed water and CO₂). Upon arrival at the processing facility in Earth orbit, gentle heating of the clathrate hydrate to release CO₂ gas from liquid water (at approximately 275 K), allowing good separation of the two. Alternatively, CO₂ and H₂O could be carried separately as their pure ices. Passive thermal control should suffice for this purpose. In order to manufacture storable fuels and oxidizer, it is essential that a large quantity of water be electrolyzed into gaseous hydrogen and oxygen. It is highly desirable that liquefaction of these gases be avoided, and that the system be designed in such a way that there will be no need to accumulate large masses (volumes) of these gases. For that reason, a continuous-flow processing system is far more attractive than batch processing. This material is for use as the feedstock for manufacture of storable rocket propellants in an appropriate Earth orbit processing facility. This facility should be in an orbit chosen for relative ease of access to and from Earth, the Moon, Low Earth Orbit, and Geosynchronous Orbit, such as a Moon-resonant Highly Eccentric Earth Orbit or a lunar libration point. Some mass of completely unprocessed regolith should also be returned for use as scientific samples and as experimental feedstock for further development and refinement of processing techniques. Notionally, we choose to assume a payload of 100 tonnes of clathrate and 1 tonne of regolith. Depending on the choice of asteroid, 50-100 tonnes of H₂O may be required as the SPS propellant for the return trip.

Some of the water is electrolyzed to release hydrogen and oxygen gases, which are used directly (not stored cryogenically) in the ensuing process steps to manufacture storable fuel and oxidizer. Schematically,



Step E involves warming the hydrate to release the CO₂ as a gas and leave liquid water, and step F is essential for both fuel and oxidizer production.

As discussed earlier, if SO₂ removal at asteroid is not successful a small but poorly known fraction of the oxygen produced by electrolysis of water could be used to oxidize any gaseous sulfur compounds to SO₃, which can be removed by a wet scrubber, another familiar terrestrial mineral-industry technology. This oxidation process would also destroy any residual traces of ammonia and produce molecular nitrogen. The sulfuric acid produced in the scrubber is a valuable commodity that must be stored for future use, since the availability of sulfuric acid enables a wide range of mineral processing schemes. It is also an appealing idea to stockpile the nitrogen gas for immediate use as a background recirculating gas in the processor, as well as to allow future use as a fire suppressant in habitats and as a source of hydroponic nutrients.

However, the overwhelming majority of the electrolysis products are dedicated to the hydrogen reduction of CO₂ to manufacture methanol and dimethyl ether and to the manufacture of H₂O₂ from hydrogen and oxygen.

After delivery to HEEO the more complicated processing stage, the manufacture of storable liquid fuel and oxidizer, will occur.

The HEEO processing activities (Area 3) have been modeled by DSI collaborator Sam Spencer in considerable detail, as the following flow chart illustrates. The scenario presented here avoids sulfur dioxide production at the asteroid (and hence produces limited CO₂ there) by keeping calciner temperatures low at the asteroid and transporting asteroidal solids to HEEO for roasting there. This is one of many alternatives studied to date, and reflects the highest complexity of the HEEO processing hardware to illustrate how several of the problems that may arise (no S removal at the asteroid; inability to get high H₂+CO₂ conversion to DME) could be solved.

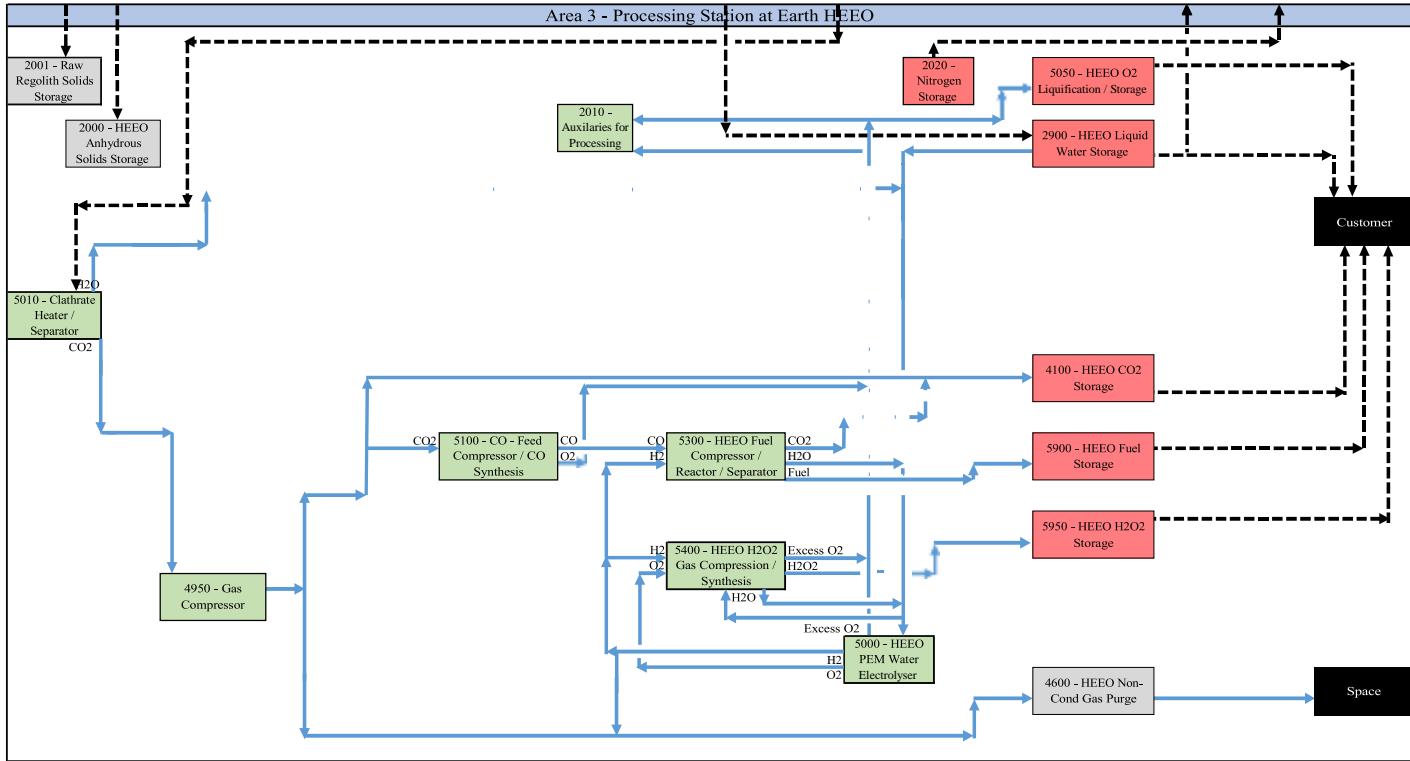


Fig. 8 The synthesis of HTP and a fuel (TBD) will be conducted in Earth orbit.

- Area 3 – Processing Station at Earth HEEO:
 - Unit 5010 – Clathrate Heater:
 - The clathrate can be heated to release CO₂ and H₂O, with re-condensation of H₂O conducted to recover reasonably clean water (with some dissolved CO₂) and a clean CO₂ gas stream.
 - Unit 4950 – Gas Compressor:
 - A simple gas compressor to provide pressure to the system.
 - Unit 5000 – PEM Electrolyzer:
 - To produce H₂ and O₂
 - Unit 5100 – CO Synthesis:
 - A Solid Oxide Electrolyzer (SOE) can be used to convert CO₂ to CO and O₂ (analogue testing completed by NASA, to be tested in-situ on 2020 Mars mission)
 - Unit 5300 – DME / MeOH Synthesis:
 - CO and H₂ can be used to produce Dimethyl Ether (DME) or Methanol via direct synthesis
 - Unit 5400 – H₂O₂ Synthesis:
 - H₂O₂ can be produced from the available H₂ and O₂ gases using direct synthesis

Combination Sabatier/SOE units may be worthwhile and have been examined and tested by various private enterprises, one example is from Paragon Space Development Corporation: <http://ntrs.nasa.gov/archive/nasa/casi.ntrs.nasa.gov/20140009943.pdf>.

The results from this analysis and process simulation can be seen identified below All calculations are based on asteroid 2009 HC orbit and assumed CI asteroid composition.

Table 3. Analysis of producing different fuels for use with HTP.

Description	Units	Case F (DME- H2O2) [regolith to HEEO]	Case G (Clathrate- DME- H2O2)	Case H (Clathrate- Ethanol- H2O2)	Case I (Clathrate- Methanol- H2O2)	Case J (Clathrate- Ethylene- H2O2)
Water delivered to HEEO	t/period	30.0t	8.0t	8.0t	8.0t	8.0t
Final Water available at HEEO after processing	t/period	0.5t	0.2t	0.5t	0.2t	4.0t
Fuel Production at HEEO, as GJ of combustion with specified Oxidizer	GJ/period	79GJ	342GJ	341GJ	384GJ	383GJ
Final CO2 available at HEEO after processing	t/period	4.5t	2.4t	1.0t	0.8t	0.2t
Energy Requirements						
MAX Thermal Energy (limit = 100kW)	kW	98 kW	92 kW	92 kW	92 kW	92 kW
Solar Mirror Area	m ²	149 m ²	140 m ²	140 m ²	140 m ²	140 m ²
MAX Electrical Energy (limit = 40kW)	kW	22 kW	26 kW	26 kW	26 kW	26 kW
Photovoltaic Cell Area	m ²	80 m ²	93 m ²	93 m ²	93 m ²	93 m ²
MAX Energy Removal	kW	59 kW	106 kW	106 kW	106 kW	106 kW
Radiator Area	m ²	179 m ²	321 m ²	321 m ²	321 m ²	321 m ²
Propulsion						
Thrust Time from Asteroid to HEEO with Cargo (includes 10% time margin, limit = 50-70%)	% of total time	69%	49%	49%	49%	49%
Specific Thrust (includes 10% time margin)	mN/kW	369 mN/kW	369 mN/kW	369 mN/kW	369 mN/kW	369 mN/kW
TOTAL Weight of Harvester to Asteroid (limit = 15.6t)	t	13.7 t	13.7 t	13.7 t	13.7 t	13.7 t
TOTAL Weight of Harvester to HEEO	t	361 t	212 t	212 t	212 t	212 t

These results indicate the following:

- The effectiveness of clathrate in maximizing fuel production at HEEO for the same transport energy from asteroid

- Even though Methanol has a lower heat of combustion (see Section 15) as higher tonnages are produced the overall energy for propulsion available is greater than for DME/Ethanol.

18. Hydrogen peroxide as a monopropellant

Although the main thrust of this study is to assess the coproduction of HTP and DME as storable bipropellants, it is clear that HTP alone can be used as a storable monopropellant providing a specific impulse of about 160 seconds. HTP has the added virtue that it is far safer to handle than hydrazine or its derivatives.

Since HTP synthesis requires only water as a starting material, it may be manufactured in Earth orbit without any requirement for carbon dioxide retrieval. HTP would be a very simple and useful propellant for small spacecraft.

19. Applications of this Propellant Manufacturing Scheme: the Mars System and the Moon

Mars: Proposed schemes for the manufacture of propellants on the surface of Mars make use of local atmospheric CO₂, which is reacted with hydrogen imported from Earth to manufacture methane via the Sabatier process. However, fully half the surface area of Mars carries a permafrost layer that is rich in water. The use of local water and CO₂ removes the necessity for importation of the deep cryogen liquid hydrogen, which involves many months of refrigerated storage of voluminous and heavily insulated liquid hydrogen tanks in space en route to Mars. The propellant production scheme we propose here requires only CO₂, water, and power. Once installed on Mars, it can function autonomously, continuing to manufacture propellant and oxidizer without cryogenics or any further resupply from Earth.

Phobos and Deimos: The two Martian moons are of spectral type D, suggestive of short-period comet nuclei, and consistent with the carbonaceous Tagish Lake meteorite, but without evidence of a water signature in the 3 μ m region. A plausible explanation is that Ph/D were captured as volatile-rich bodies similar to comet nuclei, but aeons of collisional shock heating and reaccretion of the heated ejecta has led to severe depletion of volatiles such as water in the regoliths of these bodies. The steep gravitational potential gradient in the vicinity of the orbits of Ph/D favors efficient reaccretion of ejecta from orbiting debris bands, a phenomenon of negligible importance for asteroids. The interiors of both bodies, protected from shock heating, may still be volatile-rich, but present data do not allow any firm conclusions. If an exploratory mission discovers strong evidence for a water-bearing interior in either body, both would become credible locations for

storable propellant production. Even in the absence of spectral evidence for water, involatile organic polymers and magnetite very likely coexist in the surface regions of Ph/D. Strong heating of this assemblage would release carbon dioxide, water vapor, and nitrogen. The presence of 3 wt% organic polymer implies about 0.3 % H, which upon oxidation by magnetite would generate 2.7% water. The importance of Mars missions in current long-range planning suggests a potential high importance for resource evaluation and extraction missions to these satellites.

Moon: Present techniques for detecting volatiles in the lunar polar regions are appropriate for detection of hydrogen compounds but insensitive to carbon dioxide. Nonetheless, since the volatiles in the lunar polar deposits are derived from cometary and asteroidal impactors, it is a virtual certainty that CO₂ will be an important constituent, probably the second most abundant compound in the ice deposits. If some means of mining and separating lunar polar ice can be devised and made to function efficiently under the extremely hostile local conditions (temperatures close to 50 K; total darkness; extremely hard-frozen permafrost; ubiquitous highly abrasive glassy shards in the regolith), then the two essential ingredients for in-space storable propellant manufacture would be available. Launches from the lunar surface to Low Lunar Orbit (LLO) and to the lunar Lagrange points would be possible without any reliance on either propellant resupply from Earth or on production, storage, and refrigeration of cryogenes.

20. Mission Opportunities for Use of Storable Space-based Propellants

Several transportation elements come together to enable delivery of propellant to customers in various Earth-orbit destinations from resources extracted from NEAs, and those elements are described here.

First, the Harvester spacecraft will transport resources to Earth's vicinity from a NEA using STP with water, processed from a portion of the resources extracted from the NEA, as propellant. Transportation of the Harvester spacecraft from HEEO to NEA, carrying excavation and water extraction equipment, is also part of the overall scenario. But it is a much smaller and less constraining part of the picture, and isn't explicitly described in this section, except briefly in Section 20.4.

Second, the Harvester is captured into the Earth orbit in which the HEEO Processing Facility resides. The current baseline is capture via a single lunar swingby.

Third, a HEEO is selected for the Processing and Storage Facility that is accessible from a wide enough range of NEA sources, is accessible to key customer destinations in Earth orbit, and is adequately stable over time under influences such as lunar and solar perturbation.

Fourth, transportation to customer destinations in Earth orbit. Destinations considered thus far are LEO (including staging for Mars missions), GTO, GEO, and direct injection to Mars or other heliocentric destinations from the HEEO Facility orbit or from other HEEO staging orbits.

20.1 Transportation from NEAs to Earth's vicinity.

Most of the storable propellants for customer use are best processed at the HEEO Facility, as described in this report. However, propellant for use in transportation from the NEA to Earth must be produced while the Harvestor spacecraft is still at the NEA, and the process must thus be less complex and energy-intensive than those envisioned for HEEO. STP utilizing water produced at the NEA has been selected, with an operating temperature high enough to provide a propulsive I_{sp} of 200 seconds. Though some of the propellant products described herein have higher performance in terms of I_{sp} , the system currently selected for transportation from the NEA to Earth nevertheless delivers to the HEEO Facility a sizable fraction of the payload extracted at the NEA. Payload fraction delivered to HEEO also has a dependence on the thrust level available, with a stronger dependence on this parameter for NEA sources that have more eccentric orbits, and thus significantly lower power and thrust available near aphelion. Follow-on analysis will optimize such parameters as thrust level and operating temperature for the STP to maximize the payload fraction delivered to HEEO for as wide a range of NEA sources as possible. A possible outcome is that such parameters may need to be tailored (within limits) for each NEA mission opportunity.

Two NEAs were examined, from a mission analysis perspective, for this study. It is expected that, with further analysis, many targets that yield greater mass delivered to HEEO (as a proportion of that departing from the NEA) will be identified. But these two serve to identify a number of issues pertaining to the wider class of targets that each represents. One of them, 2009 HC, exemplifies NEAs with semimajor axis close to that of Earth and fairly low eccentricity, so that available power and thrust remain near their 1 AU levels. The propulsive requirements are relatively benign during the mission opportunity shown but, due to the long synodic period relative to Earth, the favorable "season" for visitation by Harvestor and possible pre-cursors is fairly short, with many years between good phasing conditions. Thus the prospect of repeated visits, with possible placement of infrastructure at the NEA to support multiple visits, is less viable than for other classes of NEA.

The other NEA examined, 1998 KY26, has somewhat greater semimajor axis and eccentricity. It has correspondingly greater propulsive requirements for delivery to HEEO and, with aphelion close to 1.5 AU, lower power and thrust availability in that region of its orbit drive the desirability for higher thrust levels (than for 2009 HC) so that most of the orbit changing can be effected while the spacecraft is closer to 1 AU. The lower synodic period with Earth, though, means this is a better candidate for repeated visits, with possible infrastructure emplacement. These two examples span an important range of NEA target orbital characteristics, but the examination will be expanded in follow-on analysis. Both of these NEAs also have heliocentric inclination less than 4° . As discussed in Section 20.2, this inclination may be a practical limit in scenarios where capture to HEEO via lunar swingby is utilized.

JPL's MALTO (Mission-Analysis Low-Thrust Optimization) software was used to model the STP system for the heliocentric return trajectory from the NEA to Earth's vicinity. For 2009 HC it is instructive to show the ballistic trajectory that served as a starting point. Figure 9 shows the two-point boundary value solution (Lambert's Problem) for dates given by the NASA Ames' Trajectory Browser utility to minimize total ΔV . It is seen that an impulsive ΔV at the asteroid of 110 m/s suffices to initiate the transfer that reaches Earth on the specified date. Corresponding modeling of the STP system shows that under 15 tonnes of propellant is used, over about 50 days, to push away from the asteroid and establish a trajectory reaching Earth with no further propellant usage, such that 94% of the departing payload is delivered to Earth's vicinity. The problem is that the Earth-approach V_∞ is too high, 3.66 km/s, to allow capture at Earth. When the Earth-approach V_∞ is constrained to a lower magnitude, then it is seen in Figure 10 that the vast majority of propellant is used to reduce the Earth-approach V_∞ to that constrained level. Here the V_∞ magnitude is limited to 1.5 km/s, which represents the most that can likely be removed through lunar swingby, per the discussion of Section 20.2. But that results in only 27% of the initial propellant load being delivered to Earth's vicinity.

Figure 11 depicts the modeling, using MALTO, of the Harvestor spacecraft returning from 1998 KY26. As in Figure 10, return from 2009 HC, the Earth-approach V_∞ is constrained to be reduced to 1.5 km/s, which results in most of the propellant payload being used for this purpose during the transfer. As discussed above the greater aphelion of this NEA target and transfer orbit means that much less power and thrust are available at those distances. The optimal trajectory thereby concentrates much of the orbit adjustment to the period immediately preceding Earth approach (i.e., near 1 AU). When the maximum thrust level was set to half the level used in the scenario of Figure 11, then thrusting was required during the entire transfer orbit (including portions where it was likely fairly ineffective) and the payload fraction returned to Earth vicinity was significantly lower than that shown here.

Although increase of the STP I_{sp} beyond that used here of 200 seconds may not be practical due to temperature limitations, these results indicate that appropriate sizing of the power and thrust levels will be important for being able to return acceptable fractions of the payload from a sufficiently wide range of NEA targets.

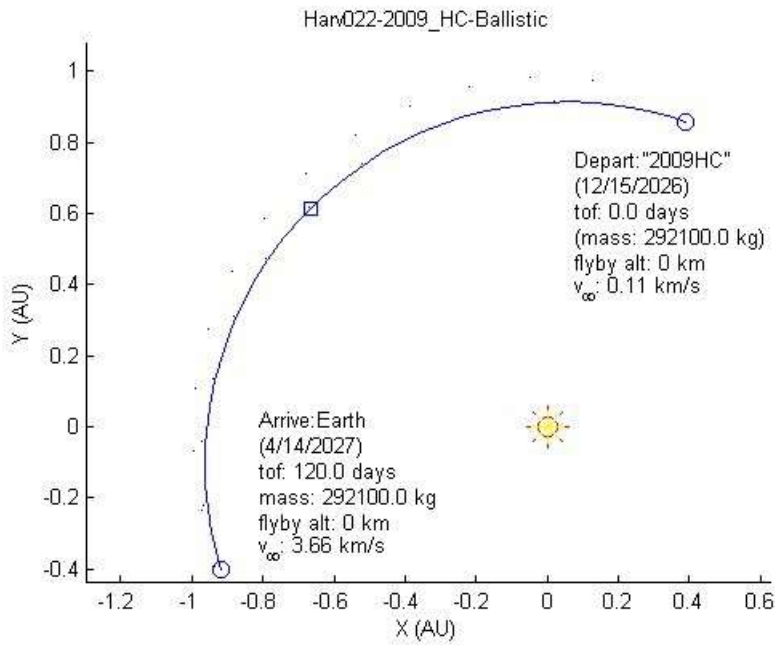


Fig. 9 Ballistic Trajectory between 2009 HC and Earth.

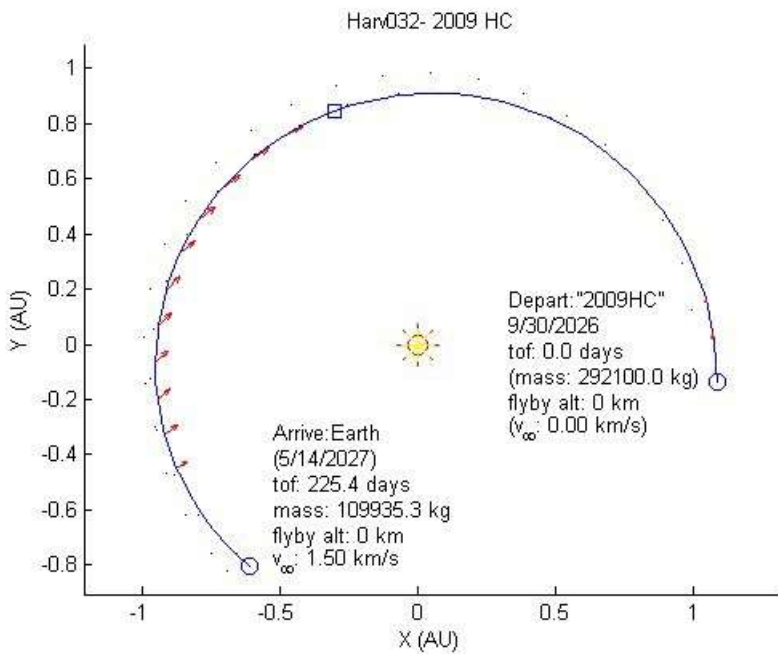


Fig. 10 STP transfer between 2009 HC and Earth. $I_{sp} = 200 \text{ s}$, Thrust = 45N @ 1 AU

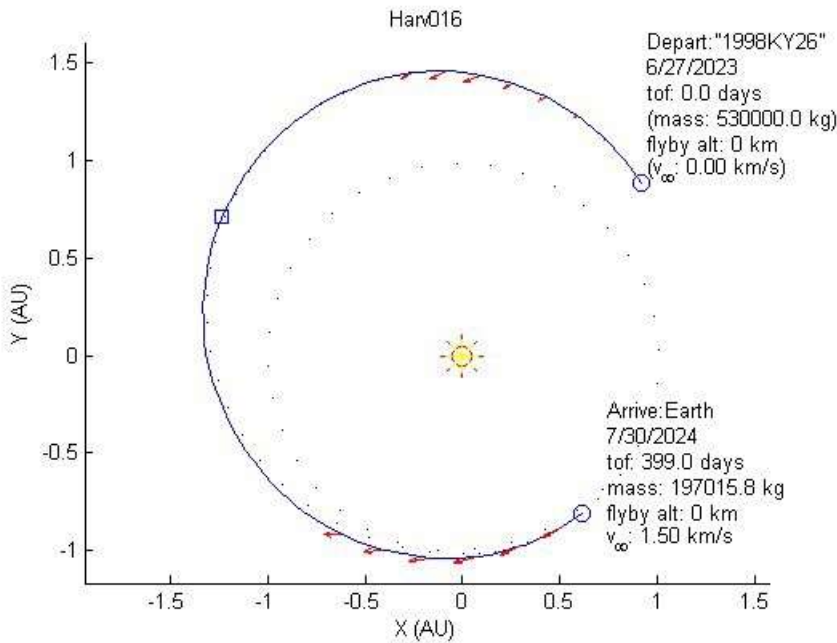


Fig. 11 STP transfer between 1998 KY26 and Earth. $I_{sp} = 200$ s, Thrust = 80N @ 1 AU

20.2 Capture and delivery to HEEEO Processing Facility orbit via single lunar swingby.

Though the modeling shown in the section above shows a large portion of the payload being expended to reduce the V_{∞} approaching Earth to lower levels, the returned payload would be far smaller still if the STP system were required to reduce V_{∞} all the way to zero, or yet further to a negative $C3$ (i.e., capture by Earth; $C3 = V_{inf}^2$). Thankfully, the presence of Earth's Moon provides a mechanism, though limited, for effecting such reduction without propellant expenditure.

Other, simpler, mechanisms also exist for capture into Earth orbit including propulsive braking close to the Earth that takes advantage of the multiplying benefit of the Oberth effect, and also aerocapture into Earth orbit. Propulsive braking, utilizing the Oberth effect, must be conducted while the spacecraft is very close to Earth, and at the speeds involved this means the maneuver must be performed within tens of minutes around perigee. Given the high mass and low thrust available this is impractical. Aerocapture utilizes a passage through the Earth's upper atmosphere (around 100 km altitude TBC) to lose enough energy to be captured into Earth orbit in a single such passage through aerodynamic drag. A single passage is all you get else you escape again into heliocentric space. But for the amount of energy to be shed, protection of the payload with an aeroshell and/or other mass increases for structural and thermal protection, will be necessary. Aeroshells may be constructed from asteroid material, and the material thereof will itself be valuable in space. Aeroshells are thus very much a part of a robust and mature space resources economy, but in the early stages addressed in this scenario represent an unneeded complexity and

risk factor. Also, aerocapture may be untenable politically due to the risk to the Earth, whether real or perceived, of passing large masses through the Earth's upper atmosphere. It should be noted that while aerocapture is not advocated for this early space resource utilization scenario aerobraking, as a facilitator of delivery of processed propellants to lower orbits, is advocated as described in Section 20.4. Aerobraking is distinguished from aerocapture by upper atmospheric passes for energy reduction after the spacecraft has been captured into Earth orbit. Since the spacecraft is already captured, aerobraking passes can be arbitrarily gentle, i.e., little or no mass added for structural or thermal protection by breaking the energy reduction up into multiple perigee passes. That, however, comes at the expense of added mission duration.

Figure 12 depicts the modeling of the capture from heliocentric space into HEEO via lunar swingby. AGI's STK software (Systems ToolKit, formerly Satellite ToolKit) was used for this modeling and targeting. A leading-edge lunar swingby was targeted to maximize the Earth-approach V-infinity that is removed by the swingby, without being specific to a particular asteroid starting point. The swingby targeting described below resulted in a maximum approach V-infinity of 1.53 km/s ($C3 = +2.34 \text{ km}^2/\text{s}^2$) that was captured to the prescribed HEEO. The heliocentric approach orbit had a very low inclination, though, of about 0.1 degrees. Asteroid-specific approach

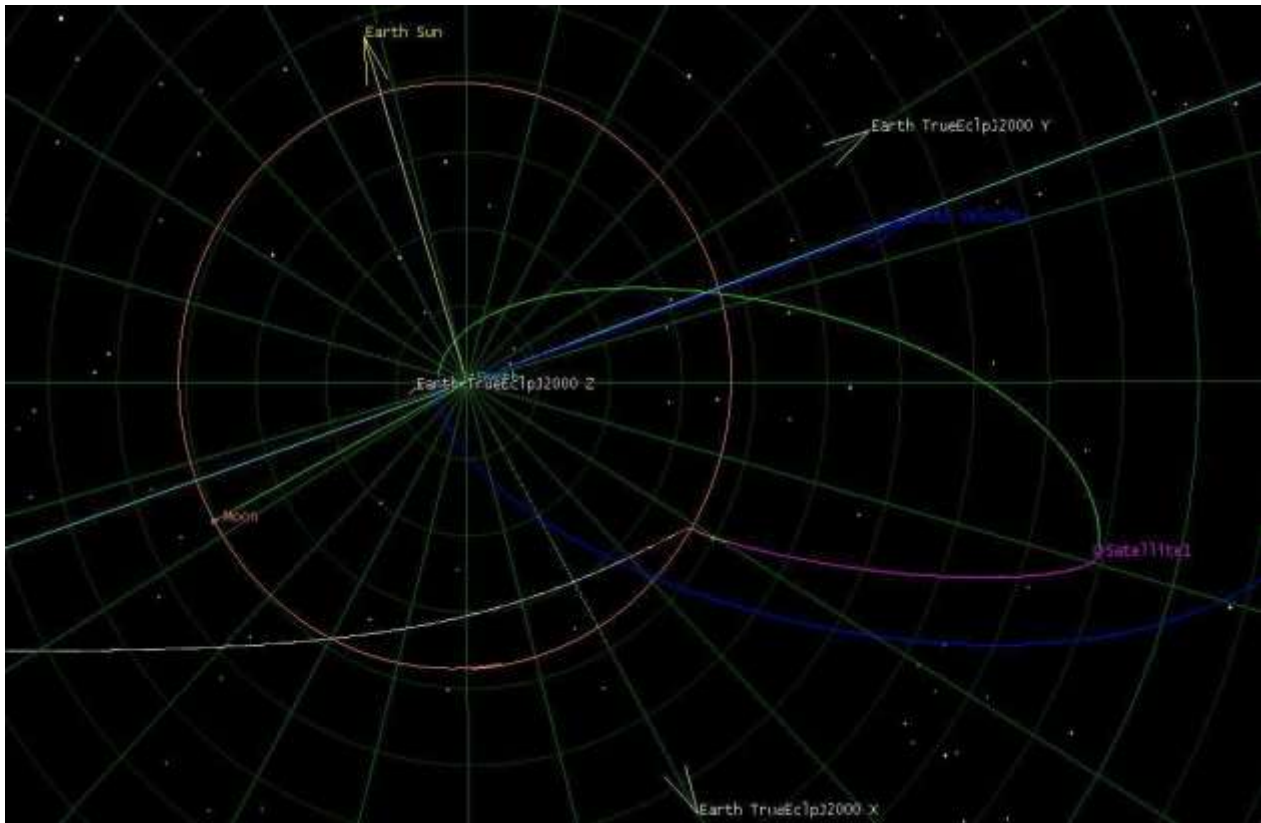


Fig. 12. Lunar swingby trajectory. The returning spacecraft enters the frame from the bottom left (white line) before passing ahead of the Moon (violet then green and blue lines) to swing into a HEEO with apparently reasonable access to the GEO belt, and outgoing NASA missions to Mars and the outer planets.

trajectories (individually and as classes of asteroid orbit), and the conditions and limits these place on the swingby benefit, will be developed further in Phase II. The spacecraft approaches the leading edge of the Moon from the Earthward side, and the perilune is constrained to be no lower than 100 km above the Moon's surface. The swingby conditions are adjusted to achieve two conditions at the first post-swingby apogee. At first apogee these conditions are that the distance from Earth is 1.0 Mkm (or about $C3 = -0.8 \text{ km}^2/\text{s}^2$) and that apogee coincides with crossing of the Earth's equatorial plane. The latter condition facilitates use of a maneuver at apogee to rotate the spacecraft orbit plane into the Earth's equatorial plane, since that is the currently desired plane for the HEEO Facility. The apogee maneuver is also simultaneously used to change perigee to any desired value. The resulting HEEO has low perigee and very high apogee; to establish the current baseline HEEO Facility orbit a maneuver of 153 m/s at the first apogee after the lunar swingby was applied to both rotate the orbit inclination into the equatorial plane, and to raise perigee from 722 km to 36086 km (GEO +300 km) altitude. Though this maneuver is on the large side for this heavily-laden low-thrust spacecraft, the velocity near this apogee is low enough that most of the thrusting can be concentrated near apogee where it is most effective. A maneuver at the following perigee of 27 m/s then lowers apogee so that a period of 27.3 days is established for 1:1 resonance with the Moon's orbit. The two-body state of the orbit at this perigee is then taken to be that of the HEEO Facility orbit, for purpose of the transfer calculations for various propellant customer destinations shown in Section 20.4.

As noted above, the lunar swingby modeled here is not specific to the approach trajectory from a particular NEA target. There may be other approach geometries that result in capture into favorable (but different) HEEO Facility orbits, and many other approach geometries for which lunar swingby capture doesn't work well at all. One determining factor is the Sun-Earth-Moon angle (or lunar phase) at the time that the Harvestor approaches the Earth-Moon system. The Earth-approach date that is optimal for the heliocentric transfer (as determined here by MALTO) may not have good geometry for lunar swingby capture. One may have to change the Earth-approach date by plus or minus half a lunar period (+/- 14 days) to change the swingby conditions to ones that are usable, and that will come at some cost of some reduction of optimality of the heliocentric portion. For NEA targets with very low inclination, that change in Earth-approach date can be made with little penalty. For targets with higher inclinations, and modeling thus far suggest 4 degrees may be an upper bound, shifting the Earth-approach date comes with greater penalty. Besides inflexibility in shifting the Earth-approach date, another factor working against high inclination approaches is that lunar swingby capture is most effective (allows the most energy reduction) when conducted close to the Earth-Moon orbit plane (which is about 9 degrees from the ecliptic plane). Thus, for higher inclination NEAs, some of the payload may also be needed to be expended to reduce the z-component of the approach V-infinity, and not just the total magnitude of V-infinity. Despite these complexities and limitations, the alternative of using payload expenditure all the way to capture instead of lunar swingby, will usually result in less payload delivered to the HEEO Facility orbit.

There are other lunar swingby geometries that may work on Earth-approach dates when the geometry described here won't, thus potentially reducing the shifting needed of the Earth-approach date. This includes, but isn't limited to, a close approach to Earth followed by lunar swingby capture. While tempting to do some propulsive braking at perigee to make use of the Oberth effect, the high speed of the perigee passage combined with the high-mass low-thrust condition of the Harvester make the effectiveness of such braking limited. There are multiple lunar swingby geometries (sometimes connected by a high-apogee solar-perturbed loop) that can increase effectiveness beyond that which can be obtained through a single lunar swingby. Though these should be explored they add to the complexity and, more importantly, to the mission duration before payload is delivered to the HEEO Processing Facility.

20.3 Selection of the HEEO Processing and Storage Facility Orbit

There is a strong business incentive to have a single Earth-orbit facility for resource processing and storage. That orbit must be adequately accessible both to Harvester spacecraft escaping toward and returning from NEA destinations, as well as to the customer markets that the processed propellants serve. The current baseline HEEO Facility orbit has many positive aspects toward that end. To summarize, the low perigee, just above the GEO belt (GEO+300km), keeps the HEEO Facility out of the worst radiation of the Van Allen belts while keeping close to GEO customers. Further analysis in Phase II could show the perigee should be somewhat higher for adequate radiation protection. The trade between stability and orbit maintenance cost could also lead to selection of a higher baseline perigee since the HEEO, as currently chosen, is subject to some fluctuation of the perigee (and apogee) due to natural perturbations (mainly lunar and solar).

The high apogee of the HEEO makes small the cost of changing perigee to that of LEO, GTO or GEO customers through apogee maneuvers, or to lower perigee to an altitude where aerobraking may be employed. The period of the HEEO, currently in 1:1 resonance with that of the Moon, allows for long-term stability despite the high apogee if the line of apsides is sufficiently displaced from the Moon's location. The choice of resonance ratio of the period with that of the Moon and the needed displacement of the line of apsides from the Moon's direction need to be part of examination of its stability and maintenance cost that should be explored further in Phase II. Also to be explored further is whether other possible HEEO choices are as readily accessible as this 1:1 resonance with the Moon choice after the lunar swingby capture. Related to that is the phasing of the HEEO line of apsides away from the Moon's direction. The propulsive cost of that could be small or zero by breaking up the post-lunar swingby maneuvers into multiple ones. But if this phasing takes several orbit periods then the time cost of this phasing could be prohibitive.

Having the HEEO Facility orbit in the equatorial plane serves GEO customers well, as well as many customer service points in GTO and LEO. It may or may not serve NASA plans well for orbital staging of propellant for Mars missions, whether that staging be in LEO or a different

HEEO. If this need by NASA is the primary user of this scenario then that would drive the choice of HEEO Processing orbit to meet that need. Otherwise, a balance will need to be made in this orbit choice in order to best meet the needs of all users in a cost-effective way. Eventually, if and when the market bears, the best solution may be multiple HEEO Facilities in different HEEOs meeting the needs of disparate users of asteroid-derived propellant.

20.4 Delivery of processed propellants to customer orbits.

Table 4 shows Delta-Velocities, modeled impulsively in a two-body framework, to transfer from the HEEO Facility orbit to various destinations. The first row (a) is part of the scenario for resource extraction from an asteroid and would likely use STP at $I_{sp} = 200s$, since that is baselined for the return leg in that scenario. The other rows (b-f) are all scenarios for delivery of processed storable propellants from the HEEO Facility to the indicated customer destinations. As such, use of processed propellant to effect the ΔV s for those rows in the table could give better performance than does STP.

Table 4. ΔV costs (impulsively modeled) for delivery of HEEO materials to markets in other orbits.

HEEO Processing Facility To:	All-Propulsive (km/s)	With Aerobraking (km/s)
a) Harvester to 2009 HC Rendezvous	0.894	N/A
b) Direct Injection to Mars ($C3=15 \text{ km}^2/\text{s}^2$)	0.853	N/A
c) NASA HEO Staging for Mars	0.190	0.152
d) NASA LEO Staging for Mars	3.319	0.229
e) GTO (550 km perigee)	0.880	0.193
f) GEO	1.153	1.634

The aerobraking option assumes perigee is reduced propulsively to 120 km altitude for aerodynamic drag effect. Energy is then dissipated perfectly at this altitude until apogee is reduced to desired level. Perigee is then raised with propulsive maneuvers at this apogee until desired final perigee is reached. Aerobraking is assumed done “gently”, possibly over several perigee passes, with no requirement for an aeroshell or other mass increases to improve structural or thermal properties.

Destination parameters for Table 4 are further described as:

- a) Harvester to 2009 HC Rendezvous: This is the outbound rendezvous opportunity with 2009 HC that corresponds to the return mission depicted in Section 20.1. The mission

opportunity map (“porkchop” plot) for this is shown in Fig. 20.5 and the minimum total ΔV from that of 0.852 km/s (= 0.646 Earth-departure + 0.206 Rendezvous) is used in the table. The Earth-departure ΔV includes a maneuver at HEEO apogee to lower perigee to 100 km and thereby make better use of the Oberth effect for injection. Since the Harvestor is very lightly loaded, compared to the return leg, the impulsive modeling here is likely a good approximation. The HEEO orbit is assumed ideally oriented for the injection, so there is likely some additional time and maneuvering not modeled to orient and phase the orbit as needed.

- b) Direct Injection to Mars: Similar to injection to the NEA describes in (a) with perigee reduction to 100 km for injection and likely additional need to re-orient the orbit. Capture at Mars is not included in the table entry.
- c) NASA HEO Staging for Mars: The NASA Mars Design Reference Architecture 5.0 shows a propellant staging option in a High-Earth Orbit with an eccentric 10-day period, LEO perigee (here assumed to be 400 km) and apogee crossing lunar distance. Table values assume the HEEO Processing Facility orbit and this HEO Staging orbit are co-planar and have apsidal lines aligned. This might be possible, per discussion above, though it seems unlikely that these orbits would coincide exactly (driving the corresponding table entries to zero) since the HEEO Facility orbit, as currently envisioned, would keep perigee orbit much higher than the staging orbit for long-term stability and radiation protection. For HEO staging, the aerobraking option is shown in the table to be lower than that for all-propulsive by 38 m/s. With this fairly small level of improvement the all-propulsive option may be preferred to avoid cost, operations, and risk issues. Still, with an all-propulsive cost shown of under 200 m/s, this seems a potentially viable alternative to launching propellant from Earth’s surface to the staging orbit.
- d) NASA LEO Staging for Mars: The NASA Mars Design Reference Architecture 5.0 shows a propellant staging option in LEO (here assumed to be 400 km). The all-propulsive option is prohibitive, consisting almost entirely of the large maneuver at LEO altitude to lower apogee from HEEO to LEO. However, aerobraking (as modeled) all but eliminates that maneuver, though it should be examined in Phase II whether energy reduction of this magnitude can be done without significant mass increases to protect against structural and thermal stresses to the payload. If it can, then bringing propellant from HEEO to the staging orbit in LEO becomes not much more expensive than bringing it to the staging orbit in HEO. Providing asteroid-derived propellants to a staging point much deeper in Earth’s gravity well (LEO vs. HEO) thereby offers potential for considerable savings in the net mass that must be launched from Earth.

Though not included in Table 4, the cost of changing inclination to that of a LEO customer is straight-forward and fairly modest, as long as the LEO destination is nearly circular. For

the current HEEO Facility baseline, an inclination change maneuver at apogee costs 4.3 m/s for a degree of change, and 122 m/s for a 28.5 degree change. That, however, would be combined orthogonally with the perigee-lowering maneuver for a smaller net cost. Thus, if the LEO Staging orbit at 400 km is equatorial like the HEEO Facility then the cost is as shown in Table 4. If the LEO orbit has an inclination of 28.5 degrees, then about 44 m/s is added to each of the options shown for LEO delivery.

- e) GTO: The aerobraking option for delivery to this destination looks quite favorable since, compared to GEO as the destination, the perigee needs to be raised only a few hundred kilometers out of the atmosphere, and not all the way to GEO. For service to satellites launched from fairly equatorial sites (such as Kourou or from ocean barges) the extra cost of inclination change will be fairly small, or will otherwise be similar to that described above when LEO is the destination. Since the GTO is quite eccentric, though, additional attention will need to be made to the alignment of the lines of apsides of the GTO destination and the HEEO Facility orbits. That may be easily handled by time constraints on the launch vehicle to GTO, rather than additional maneuvering by the vehicle making the propellant delivery from the HEEO Facility.
- f) GEO: This destination benefits, due to the current baseline selection of the HEEO Processing Facility to be in the equatorial plane, from not needing orbit adjustments beyond that modeled in Table 4. However the aerobraking option suffers, relative to an all-propulsive one, due to the high cost of raising perigee from atmospheric to GEO altitude using maneuvers at GEO. That cost could be reduced by raising perigee with maneuvers at super-synchronous altitude, but then the aerobraking benefit is also reduced. The all-propulsive cost is also relatively high and will need to be compared carefully to the alternative means of getting to GEO.

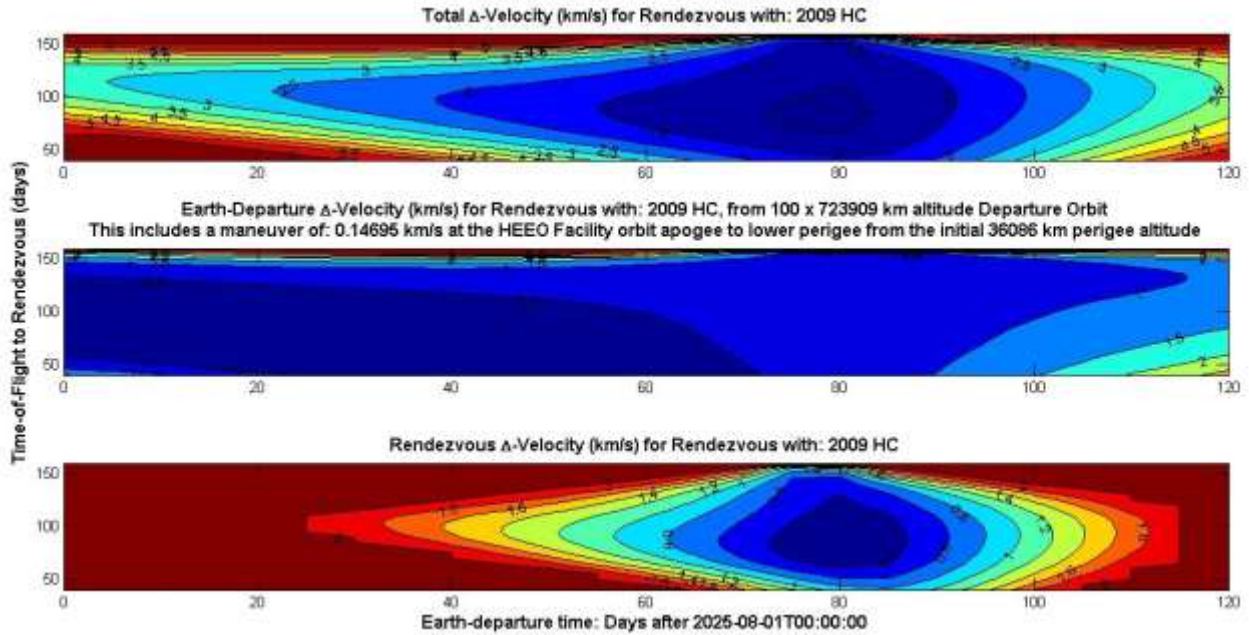


Fig. 13 “Porkchop” Plot Showing Mission Opportunity in terms of ΔV (Total, Earth Escape & Rendezvous) for Impulsive Transfer from HEEO Facility Orbit (Oct 2025) to Rendezvous with 2009 HC

A general energy-based argument suggests that the tonnage launched from Earth, for either staging in LEO or HEO orbits, should be about the same since the total energy to go from the ground to Mars-injection is about the same whether you have an intermediate staging point deep in Earth’s gravity well (LEO) or higher in the well (HEO). If that argument holds up then, and removing cost estimates from the direct comparison, one can use an estimate instead of tonnage of propellant needed at each staging orbit to inject the remaining infrastructure toward Mars. That propellant tonnage is then converted to the number of SLS launches needed to take it to the respective staging orbits. On the other side of the comparison, the tonnage of Mars injection propellant needed at each staging orbit can be expressed as a number of Harvestor payload equivalents.

Expressed just as tonnage of ground-launched propellant replaced by asteroid resources, it seems a case can be made that the asteroid-derived propellant scenario is more strongly beneficial for the LEO-staging option over the HEO one. That’s because, for a marginally greater cost of delivery of propellant to LEO vs. HEO from the HEEO Processing orbit, there is a much greater need for propellant staged in LEO (and thus greater potential for replacement of ground-launched propellant vs. asteroid-derived propellants) since the delta-V needed to inject (the rest of the way) to Mars is much greater in LEO than in HEO. However, the delivery capability of each SLS will be correspondingly much greater to the LEO staging orbit than to the HEO one. From an energetic viewpoint (again), it may be that the number of SLS launches needed to place Mars injection propellant at either staging orbit is about the same, despite the greater tonnage needed for this in

LEO. If so, then the asteroid-derived propellant scenario could be more strongly beneficial for the HEO-staging option over the LEO one since fewer Harvestor payload equivalents will be needed to serve that staging location. A more detailed examination of the parameters affecting this comparison will be made in Phase II of this study. Regardless of which Mars Mission staging orbit is selected, though, use of asteroid-derived propellant can lower the cost of the mission if the cost per tonne of propellant delivered to the needed utilization location is low enough.

21. Synergy with New-Generation Low-Cost Earth-Launch Technologies

From a national perspective, in-space production of storable propellants is the key enabler for reusable space-based transfer stages that will complete the transportation-cost revolution begun by evolving launch systems from SpaceX, Blue Origin, Stratolaunch, and others. These aim for various levels of reusability for their first stages, but reusability for a re-entering upper stage is very challenging. Space-based transfer stages neatly eliminate this problem. They also eliminate the 30-35% propellant mass carried by comsats for GTO to GEO transfer, since space-based refuelable transfer stages can deliver these comsats to GEO. A more advanced system architecture, incorporating a LEO/HEO shuttle tug with aerobraking capability, could deliver our propellants to LEO and serve the large LEO to GTO market (and possibly transfer from LEO to GPS-type orbits) as well. The combination of decreasing launch costs and in-space propellant production dramatically lowers the cost of high-orbit and beyond-Earth activities. U.S. taxpayers and commercial concerns will enjoy reduced costs for satellite-delivered communications, entertainment, navigation, and Earth-monitoring services such as weather and climate forecasting.

22. Terrestrial applications of improved H₂O₂ syntheses

There are powerful economic incentives to advance the development of the technology for direct synthesis of H₂O₂ because of its environmental benefits and simplicity: hydrogen peroxide, being free of chlorine and chlorine oxides, is the safest and “greenest” oxidizing and bleaching agent known. The fuel-cell approach pioneered by Prof. Schiffrin appears to be the most promising route for direct synthesis of HTP. Any assistance we can render to help bring this technology to maturity would have wide-spread application on Earth.

We have arranged for participation of two experimental chemical engineers, Dominic Gervasio and James Farrell, both of the Department of Chemical and Environmental Engineering of the University of Arizona, to pursue electrochemical production of hydrogen peroxide for Phase II of this work.

References

1. J.S. Lewis, Construction Materials for an SPS Constellation in Highly Eccentric Earth Orbit. *Space Power* 10, 353-362 (1991).
2. J.S. Lewis, Logistical Implications of Water Extraction from Near-Earth Asteroids. In: *Space Manufacturing* 9, AIAA, Washington D. C., 71-78 (1993).
3. P. R. Weissman, W. F. Bottke and H.F. Levinson, Evolution of Comets into Asteroids. In: *Asteroids III*, W. F. Bottke et al., eds., Univ. of Arizona Press (2002). See especially Tables 2 and 3. Also, more recently, comet rejuvenation is discussed in: I. Ferrin, et al., The 2009 Apparition of the Methuselah Comet 107P/Wilson-Harrington: A Case of Comet Rejuvenation? *Planetary and Space Science* 70, 59-72 (2012). (The name “Methuselah” is a misnomer; it should be “Lazarus”.)
4. Rosetta albedo data at: <http://blogs.esa.int/rosetta/2014/10/17/navcams-shades-of-grey/>; astronomical albedo data from J. M. Bauer, et al., WISE/NEOWISE Preliminary Analysis and Highlights of the Comet 67P/Churyumov-Gerasimenko Near Nucleus Environs, <http://arxiv.org/abs/1209.2363>.
5. JANAF Thermochemical Tables, <http://kinetics.nist.gov/janaf/>
6. E. S. Domalski, Selected Values of Heats of Combustion and Heats of Formation of Organic Compounds Containing the Elements C, H, N, O, P, and S. *J. Phys. Chem. Ref. Data* 1, 220-278 (1972).
7. R. A. Robie and B. S. Hemingway, Thermodynamic Properties of Minerals and Related Substances at 298.15 K and 1 Bar (10^5 Pascals) Pressure and Higher Temperatures, *U. S. G. S. Bulletin* 2131 (1995).
8. K. Fredriksson and J. F. Kerridge, Carbonates and Sulfates in CI chondrites: Formation by Aqueous Activity on the Parent Body. *Meteoritics* 23, 35-44 (1988).
9. D. Vaniman, D. Pettit, and G. Heiken, Uses of Lunar Sulfur. <http://www.nss.org/settlement/moon/library/LB2-509-UsesOfLunarSulfur.pdf>
10. S. Cloëz, Analyse chimique de la pierre météorique d’Orgueil, *Comptes Rendus* 59, 37-40 (1864).

11. F. Pisani, Étude chimique et analyse de l'aérolithe d'Orgueil, Seances Acad. Sci. 59, 132-135, (1864).
12. T. Nakamura, R. H. Krech, J. A. McClanahan and J. M. Shoji, Solar Thermal Propulsion for Small Spacecraft- Engineering System Development and Evaluation, 41st AIAA 2005-3923, AIAA/ASME/SAE/ASEE Joint Propulsion Conference, Tucson (2005).
13. Ultramet, Marshall SFC, and UAH work on solar thermal propulsion: Numerous citations to these projects are available in conference papers and online.
14. F. G. Kennedy, Microsatellite Maneuvering, Ph. D. Dissertation, Univ. of Surrey (2004).
15. <https://spacecraftlab.wordpress.com/author/mapeck/>
16. Hydros/Tethers Unlimited: <http://www.tethers.com/HYDROS.html>
17. ISS H₂O electrolysis: <https://www.asme.org/engineering-topics/articles/aerospace-defense/making-space-safer-with-electrolysis>
18. S. Circone, et al., CO₂ Hydrate: Synthesis, Composition, Structure, Dissociation Behavior, and a Comparison to Structure I CH₄ Hydrate. J. Phys. Chem B, (2003).
19. There is an extensive literature on commercial synthesis of methanol from CO and hydrogen. A variant of the process that seems well suited for use in space is found in: R. M. Agny and C. G. Takoudis, Catalytic Synthesis of Methanol..., available online at https://web.anl.gov/PCS/acsfuel/preprint%20archive/Files/30_2_MIAMI%20BEACH_04-85_0318.pdf
20. The use of a γ -alumina catalyst in direct synthesis of dimethyl ether (DME) is described in: <http://wiki.gekgasifier.com/w/page/6123698/Dimethyl%20Ether%20%28DME%29>
21. Andrés T. Aguayo, J. Ereña, D. Mier, J. M. Arandes, M. Olazar and J Bilbao, Kinetic Modeling of Dimethyl Ether Synthesis in a Single Step on a CuO-ZnO-Al₂O₃- γ -Al₂O₃ catalyst, Ind. Eng. Chem. Res., 46 (17), 5522-5530 (2007).
22. An, X., Zuo, Y-Z., Zhang, Q., Wang, D.-Z., and Wang J.-F., Dimethyl Ether Synthesis from CO₂ Hydrogenation on a CuO-ZnO-Al₂O₃-ZrO₂/HZSM-5 Bifunctional Catalyst. Ind. Eng. Chem. Res. 47(17), 6547-6654 (2008).
23. Huot-Marchand, P.-E., Dimethyl Ether Production from Carbon Dioxide and Hydrogen,

NTNU TPG4140, Trondheim, Norway (2010)

24. <http://www.diyspaceexploration.com/storing-hydrogen-peroxide/>
25. For an introduction to schemes for direct synthesis of hydrogen peroxide from hydrogen and oxygen, see: J. Garcia-Serna, et al., Engineering in Direct Synthesis of Hydrogen Peroxide: <http://pubs.rsc.org/en/content/articlelanding/2014/gc/c3gc41600c#!divAbstract>
26. G. Blanco-Brieva, et al., Direct Synthesis of Hydrogen Peroxide on Palladium Catalyst... <http://digital.csic.es/bitstream/10261/26339/1/C003700A.pdf>.
- 26b. J. K. Edwards, et al., Advances in Direct Synthesis of Hydrogen Peroxide from Hydrogen and Oxygen. *Catalysis Today* 248, 3 (2015).
- 26c. P. Biasi, et al., Hydrogen Peroxide Direct Synthesis: from Catalyst Preparation to Continuous Reactors. <http://www.aidic.it/icheap10/webpapers/378Biasi.pdf>
- 26d. J. K. Edwards, B. Solsona, E. Ntainjua, A. F. Carley, A. A. Herzing, C. J. Kiely, and G. J. Hutchings, Switching off Hydrogen Peroxide Hydrogenation in the Direct Synthesis Process. *Science* 323, 1037-1039 (2009).
27. Prof. Schiffrin's Patent application at: <http://www.google.com/patents/US20040053098>.
28. http://www.researchgate.net/publication/265868341_HYDROGEN_PEROXIDE_FROM_BRIDESMAID_TO_BRIDE
29. <http://www.google.com/patents/US3383174>
30. M. McPherson, Proceedings of the 2nd International Conference on Green Propellants for Space Propulsion, Cagliari, Italy. ESA SP-557 (October 2004).
31. T. Babinsky, et al., Hydrogen Peroxide. Reinhold Publishing Co., New York (1955).
32. Calculated using heats of formation from HSC v7 Thermodynamic database and simulated in SysCAD v9.2 build 135_17085.
33. NIST Chemistry WebBook, NIST Standard Reference Database Number 69, accessed 24th February 2016, available at: <http://webbook.nist.gov/chemistry/>